

# Interpolation can hurt robust generalization even when there is no noise

Konstantin Donhauser<sup>\*1</sup>, Alexandru Tifrea<sup>\*1</sup>, Michael Aerni<sup>1</sup>  
Reinhard Heckel<sup>2,3</sup> and Fanny Yang<sup>1</sup>

<sup>1</sup>*ETH Zurich*, <sup>2</sup>*Rice University*, <sup>3</sup>*Technical University of Munich*

## Abstract

Numerous recent works show that overparameterization implicitly reduces variance for min-norm interpolators and max-margin classifiers. These findings suggest that ridge regularization has vanishing benefits in high dimensions. We challenge this narrative by showing that, even in the absence of noise, avoiding interpolation through ridge regularization can significantly improve generalization. We prove this phenomenon for the robust risk of both linear regression and classification, and hence provide the first theoretical result on *robust overfitting*.

## 1 Introduction

Conventional statistical wisdom cautions the user who trains a model by minimizing a loss  $\mathcal{L}(\theta)$ : if a global minimizer achieves zero or near-zero training loss (i.e., it *interpolates*), we run the risk of overfitting (i.e., high variance) and thus suboptimal prediction performance. Instead, *regularization* is commonly used to reduce the effect of noise and to obtain an estimator with better generalization. Specifically, regularization limits model complexity and induces worse data fit, for example via an explicit penalty term  $R(\theta)$ . The resulting penalized loss  $\mathcal{L}(\theta) + \lambda R(\theta)$  explicitly imposes certain structural properties on the minimizer. This classical rationale, however, does seemingly not apply to overparameterized models: for example, large neural networks in practice exhibit good generalization performance on i.i.d. samples even if  $\mathcal{L}(\theta)$  vanishes and label noise is present [36].

Since interpolators are not unique in the overparameterized regime, it is crucial to study the specific *implicit biases* of interpolating estimators. In particular, for common losses, a large body of recent work analyzes the properties of the solutions found via gradient descent at convergence (see e.g. [12, 13, 22, 26, 27, 31, 44, 49]). For example, for linear and logistic regression, it is well-known that gradient descent converges to the min- $\ell_2$ -norm and max- $\ell_2$ -margin solutions, respectively [22, 27, 32, 49]. These interpolating estimators also minimize the respective penalized loss  $\mathcal{L}(\theta) + \lambda \|\theta\|_2^2$  in the limit of  $\lambda \rightarrow 0$  [44].

A plethora of recent papers explicitly study generalization properties on min- $\ell_2$ -norm interpolators [6, 15, 18, 23, 33, 34, 35] and max- $\ell_2$ -margin solutions [14, 34, 46], and show that the variance decreases as the overparameterization ratio increases beyond the interpolation threshold. While regularization with  $\lambda > 0$  is commonly known to reduce the risk at the interpolation threshold [23, 37], many of these works are motivated by the second descent of the double descent phenomenon [7] which suggests that regularization becomes redundant with sufficient overparameterization. Hence, previous papers focus on highly overparameterized settings where the optimal regularization parameter satisfies  $\lambda_{\text{opt}} \leq 0$  [29, 43, 54], implying that for large  $d/n$ , explicit regularization with  $\lambda > 0$  is redundant or even detrimental for generalization.

Taking a step back, this narrative originated from theoretical and experimental findings that consider the *standard* test risk with identically distributed training and test data. However, this

---

<sup>\*</sup>equal contribution. Presented at the 35th Conference on Neural Information Processing Systems (NeurIPS 2021).

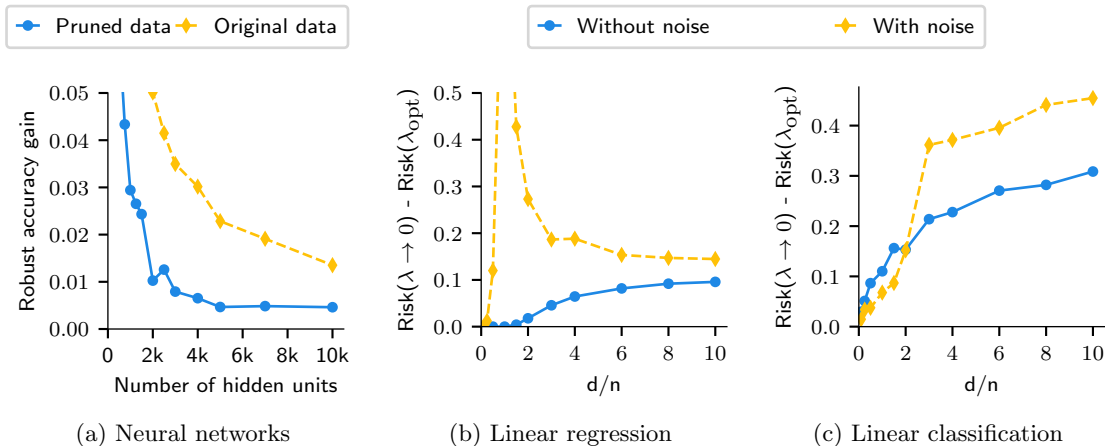


Figure 1: Avoiding interpolation can benefit robustness even in the overparameterized ( $d \gg n$ ) regime and for noiseless training data. We plot the robust accuracy gain of (a) early-stopped neural networks compared to models at convergence, fit on sanitized (binary 1-3) MNIST that arguably has minimal noise; and  $\ell_2$  regularized estimators compared to interpolators with  $\lambda \rightarrow 0$  for (b) linear regression with  $n = 10^3$  and (c) robust logistic regression with  $n = 10^3$ . See Appendix B for experimental details and Sections 3 and 4 for the precise settings of (b) and (c).

measure cannot reflect the *robust risk* of models when the test data has a shifted distribution, is attacked by adversaries, or contains many samples from minority groups [19, 21, 40, 55]. In fact, mounting empirical evidence suggests that regularization is indeed helpful for robust generalization, even in highly overparameterized regimes where the benefits for the standard risk are negligible [42]. This phenomenon is sometimes referred to as *robust overfitting*.

In the presence of noise, the following intuition holds true: since the robust risk amplifies estimation errors, its variance is larger and hence regularization – such as early stopping – can be beneficial for generalization [47]. However, we observe that even when estimating entirely noiseless signals, robust overfitting persists! We observe this phenomenon in experiments with shallow neural networks on sanitized image data depicted in Figure 1a and, in fact, even for linear models trained on high-dimensional synthetic noiseless data. In particular, Figures 1b,1c show that min- $\ell_2$ -norm and robust max- $\ell_2$ -margin interpolators (minimizers of the training loss for  $\lambda \rightarrow 0$ ), achieve a higher robust risk than the corresponding regularized estimators that do not interpolate noiseless observations (minimizers for  $\lambda > 0$ ).

To date, our observations in the noiseless case cannot be explained by prior work. On the contrary, they seem to contradict a simple intuition: if the min- $\ell_2$ -norm and robust max- $\ell_2$ -margin interpolators exhibit large risks as  $\lambda \rightarrow 0$ , the induced bias for a small  $\ell_2$ -norm is potentially suboptimal and a larger penalty weight  $\lambda > 0$  should only degrade performance. In this paper, we provide possible explanations that debunk this intuition in the high-dimensional overparameterized regime. We prove for isotropic Gaussian covariates that a strictly positive regularization parameter  $\lambda$  systematically improves robust generalization for linear and robust logistic regression. Empirically, we show that early stopping and other factors that lead to a non-interpolating estimator achieve a similar effect. Our results provide the first rigorous explanation of robust overfitting even in the absence of noise.

In Section 2, we formally define the setting that we use throughout our analysis. We then first present precise asymptotic expressions for the robust risk for linear regression in Section 3 that explicitly explain robust overfitting. Furthermore, in Section 4, we consider classification with logistic regression and derive asymptotic results.

## 2 Risk minimization framework

In this section, we introduce the data generating process that we assume throughout our analysis, and define the standard and robust risks that we use as evaluation metrics.

### 2.1 Problem setting

This paper considers the supervised learning problem of estimating a mapping from  $d$ -dimensional real-valued features  $x \in \mathbb{R}^d$  to a target  $y \in \mathcal{Y} \subseteq \mathbb{R}$  given a training set of labeled samples  $\mathcal{D} = \{(x_i, y_i)\}_{i=1}^n$ . We assume that the feature vectors  $x_i$  are drawn i.i.d. from the marginal distribution  $\mathbb{P}$  that we assume to be an isotropic Gaussian. We further focus on noiseless observations  $y_i = \langle \theta^*, x_i \rangle$  for regression tasks and  $y_i = \text{sgn}(\langle \theta^*, x_i \rangle)$  for classification tasks, respectively. However, the main results are more general and apply to noisy observations as well. For regression, we assume additive Gaussian noise with zero mean and  $\sigma^2$  variance, while for classification we flip a certain percentage of the training labels.

This paper studies the high-dimensional asymptotic regime where  $d/n \rightarrow \gamma$  as both the dimensionality  $d$  and the number of samples  $n$  tend to infinity. This high-dimensional setting is widely studied as it can often – as in our experiments – yield precise predictions for the risk of the estimator when both the input dimension and the data set size are large [9, 52]. It is also the predominant setting considered in previous theoretical works that discuss overparameterized linear models [2, 14, 15, 23, 24, 25, 50].

### 2.2 Standard and robust risk

We now introduce the standard and robust evaluation metrics for regression and classification. Given a pointwise test loss  $\ell_{\text{test}} : \mathbb{R} \times \mathbb{R} \rightarrow \mathbb{R}$ , we define the standard (population) risk of an estimator  $\hat{\theta}$  as

$$\mathbf{R}(\hat{\theta}) := \mathbb{E}_{X \sim \mathbb{P}} \ell_{\text{test}}(\langle \hat{\theta}, X \rangle, \langle \theta^*, X \rangle), \quad (1)$$

where the expectation is taken over the marginal feature distribution  $\mathbb{P}$ . Note that for any data-dependent estimator  $\hat{\theta}$ , this risk is fixed if conditioned on the training data. Our asymptotic bounds hold almost surely over draws of the training set. As standard in the literature, we choose the square loss  $\ell_{\text{test}}(u, v) = (u - v)^2$  for regression and the 0-1 loss  $\ell_{\text{test}}(u, v) = \mathbb{1}_{\text{sgn}(u) \neq \text{sgn}(v)}$  for classification.

The broad application of ML models in real-world decision-making processes increases requirements on their generalization abilities beyond i.i.d. test sets. For example, in the image domain, classifiers should be *robust* and output the same prediction for perturbations of an image that do not change the ground truth label (e.g., imperceptible  $\ell_p$ -perturbations [19]). In this case, we say the perturbations are *consistent* and the estimator that achieves zero robust population risk also has zero standard population risk. For linear models in particular, one way to enforce consistency is to restrict perturbations to the space orthogonal to the ground truth, as proposed in [41].

Motivated by the imperceptibility assumption and  $\ell_p$ -adversarial attacks widely studied in the image domain, we consider the adversarially robust risk of a parameter  $\theta$  with respect to consistent  $\ell_p$ -perturbations

$$\mathbf{R}_\epsilon(\hat{\theta}) := \mathbb{E}_{X \sim \mathbb{P}} \max_{\delta \in \mathcal{U}_p(\epsilon)} \ell_{\text{test}}(\langle \hat{\theta}, X + \delta \rangle, \langle \theta^*, X \rangle), \quad (2)$$

with the perturbation set  $\mathcal{U}_p(\epsilon) := \{\delta \in \mathbb{R}^d : \|\delta\|_p \leq \epsilon \text{ and } \langle \theta^*, \delta \rangle = 0\}$ .

In many scientific applications, security against adversarial attacks may not be the dominating concern; one may instead require estimators to be robust against small distribution shifts. Earlier work [48] has pointed out that distribution shift robustness and adversarial robustness are equivalent for losses that are convex in the parameter  $\theta$ . Similarly, in our setting, adversarial robustness against consistent  $\ell_p$ -perturbations implies distributional robustness against  $\ell_p$ -bounded mean shifts in the covariate distribution  $\mathbb{P}$  (see Appendix A.3).

### 3 Min- $\ell_2$ -norm interpolation in robust linear regression

In the context of regression, we illustrate overfitting of the robust risk in Equation (2) with the set of consistent  $\ell_2$ -perturbations  $\mathcal{U}_2(\epsilon)$ . More precisely, we show that preventing min- $\ell_2$ -norm interpolation on noiseless samples via ridge regularization improves the robust risk. Furthermore, we explain why regularization benefits the robust risk even in settings where it does not decrease the standard risk. Lastly, we note that due to the rotational invariance of the problem, our results hold for sparse and dense ground truths  $\theta^*$  alike.

#### 3.1 Interpolating and regularized estimator

We study linear ridge regression estimates defined as

$$\hat{\theta}_\lambda = \arg \min_{\theta} \frac{1}{n} \sum_{i=0}^n (y_i - \langle \theta, x_i \rangle)^2 + \lambda \|\theta\|_2^2. \quad (3)$$

The min- $\ell_2$ -norm interpolator is the limit of the linear ridge regression estimate with  $\lambda \rightarrow 0$  and is given by

$$\hat{\theta}_0 = \arg \min_{\theta} \|\theta\|_2 \quad \text{such that} \quad \langle \theta, x_i \rangle = y_i \quad \text{for all } i. \quad (4)$$

Note that the min- $\ell_2$ -norm interpolator is also the estimator that gradient descent on the unregularized loss converges to, while ridge regression with  $\lambda > 0$  corresponds to early-stopped estimators [1, 2]. Therefore, by proving that a ridge regularized estimator with  $\lambda > 0$  significantly outperforms the min- $\ell_2$ -norm interpolator with  $\lambda \rightarrow 0$ , we also show that early stopping benefits robust generalization.

Whenever the goal is to achieve a low robust risk, a popular alternative to using the standard linear regression estimate in Equations (3),(4) is to consider adversarially trained estimators [19, 25]. However,  $\ell_2$ -adversarial training in its usual form (i.e., with inconsistent perturbations) prevents regression estimators from interpolating, and hence, has a similar effect to  $\ell_2$ -regularization as we discuss in more detail in Appendix C. On the other hand, training with consistent perturbations as defined in the robust risk is equivalent to full knowledge of the direction of  $\theta^*$  and hence simply recovers the ground truth in the noiseless case. Since our goal is to reveal the shortcomings of interpolators compared to regularized estimators, we only analyze ridge estimators trained without perturbations.

#### 3.2 Robust overfitting in noiseless linear regression

The following theorem provides a precise asymptotic expression of the robust risk under consistent  $\ell_2$ -perturbations for the ridge regression estimate in Equation (3). The proof extends techniques from previous works [15, 23] based on results from random matrix theory [3, 28] and can be found in Appendix E. Without loss of generality, we can assume that  $\|\theta^*\|_2 = 1$ .

**Theorem 3.1.** *Assuming the marginal input distribution  $\mathbb{P} = \mathcal{N}(0, I_d)$ , the robust risk (2) of the estimator  $\hat{\theta}_\lambda$  for  $\lambda > 0$  (defined in (3)) with respect to consistent  $\ell_2$ -perturbations  $\mathcal{U}_2(\epsilon)$  asymptotically converges to*

$$\mathbf{R}_\epsilon(\hat{\theta}_\lambda) \xrightarrow{a.s.} \mathcal{R}_\lambda + \epsilon^2 \mathcal{P}_\lambda + \sqrt{\frac{8\epsilon^2}{\pi} \mathcal{P}_\lambda \mathcal{R}_\lambda} =: \mathcal{R}_{\epsilon, \lambda} \quad (5)$$

as  $d, n \rightarrow \infty$  with  $d/n \rightarrow \gamma$ , where  $\mathcal{P}_\lambda = \mathcal{R}_\lambda - \lambda^2(m(-\lambda))^2$  and  $\mathcal{R}_\lambda = \lambda^2 m'(-\lambda) + \sigma^2 \gamma (m(-\lambda) - \lambda m'(-\lambda))$  is the asymptotic standard risk, i.e.,  $\mathbf{R}(\hat{\theta}_\lambda) \xrightarrow{a.s.} \mathcal{R}_\lambda$ . The function  $m(z)$  is the Stieltjes transform of the Marchenko-Pastur law and is given by  $m(z) = \frac{1-\gamma-z-\sqrt{(1-\gamma-z)^2-4\gamma z}}{2\gamma z}$ . Further, the limit  $\lim_{\lambda \rightarrow 0} \mathcal{R}_{\epsilon, \lambda}$  exists for all  $\epsilon \geq 0$  and corresponds to the asymptotic standard ( $\epsilon = 0$ ) and robust risks ( $\epsilon > 0$ ) of the min- $\ell_2$ -norm interpolator  $\hat{\theta}_0$  (4).

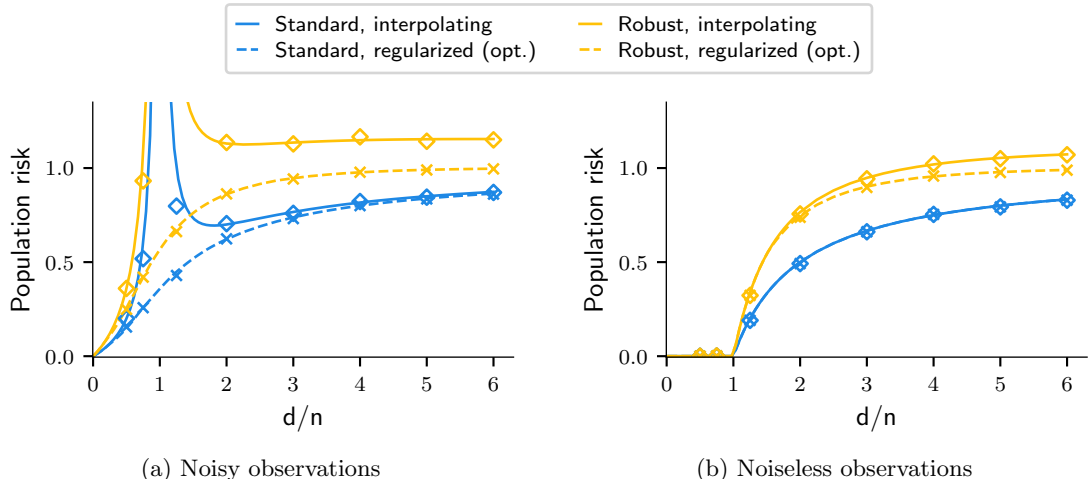


Figure 2: Asymptotic theoretical predictions for  $d, n \rightarrow \infty$  (curves) and experimental results with finite  $d$  and  $n = 10^3$  (markers) for the robust ( $\epsilon = 0.4$ ) and standard risk of the min- $\ell_2$ -norm interpolator (solid, *interpolating*) and the ridge regression estimate with optimal  $\lambda$  (dashed, *regularized*) for (a) noisy data with  $\sigma^2 = 0.2$  and (b) noiseless data. We observe that the gap between the robust risk of the interpolating and optimally regularized estimators persists even for noiseless observations.

We plot the precise asymptotic risks of the ridge estimate with optimal regularization parameter  $\lambda_{\text{opt}}$ <sup>1</sup> and of the min- $\ell_2$ -norm interpolator for  $\lambda \rightarrow 0$  in Figure 2. For the robust risk, we use  $\epsilon = 0.4$ . We first observe in Figure 2a that ridge regularization reduces the robust risk even for  $d/n \gg 1$  well beyond the interpolation threshold – the regime where previous works show that the variance is negligible, and hence, regularization does not improve generalization.

Moreover, Figure 2b illustrates that the beneficial effect of ridge regularization persists even for noiseless data. This supports our statement that regularization not only helps to reduce variance, but also reduces the part of the robust risk that is unaffected by noise in the overparameterized regime. Furthermore, we show that experiments run with finite values of  $d$  and  $n$  (depicted by the markers in Figure 2) closely match the predictions obtained from Theorem 3.1 for  $d, n \rightarrow \infty$  and  $d/n \rightarrow \gamma$ . This indicates that the high-dimensional asymptotic regime does indeed correctly predict and characterize the high-dimensional non-asymptotic regime. Finally, even though Theorem 3.1 assumes isotropic Gaussian covariates, we can extend it to more general covariance matrices following the same argument as in [23], based on results from random matrix theory [28].

### 3.3 Intuitive explanation and discussion

We now shed light on the phenomena revealed by Theorem 3.1 and Figure 2. In particular, we discuss why regularization can reduce the robust risk even in a noiseless setting and why the effect is indiscernible for the standard risk.

For this purpose, we examine the robust risk as a function of  $\lambda$ , depicted in Figure 3a for different overparameterization ratios  $\gamma > 1$  and  $\epsilon = 0.4$ . The arrows point in the direction of increasing  $\lambda$ . We observe how the minimal robust risk is achieved for a  $\lambda_{\text{opt}}$  bounded away from zero and how the optimum increases with the overparameterization ratio  $d/n \rightarrow \gamma$ , indicating that stronger regularization is needed the more overparameterized the estimator is.

In order to understand this overfitting phenomenon better, we decompose the ridge estimate  $\hat{\theta}_\lambda$  into its projection  $\Pi_{\parallel}$  onto the ground truth direction  $\theta^*$  and the projection  $\Pi_{\perp}$  onto the orthogonal complement, i.e.,  $\hat{\theta}_\lambda = \Pi_{\parallel}\hat{\theta}_\lambda + \Pi_{\perp}\hat{\theta}_\lambda$ . For the noiseless setting ( $\sigma^2 = 0$ ), substituting this

<sup>1</sup>Here we choose  $\lambda$  using the population risk oracle. In practice, one would resort to standard tools such as cross-validation techniques that also enjoy theoretical guarantees (see e.g. [38]).

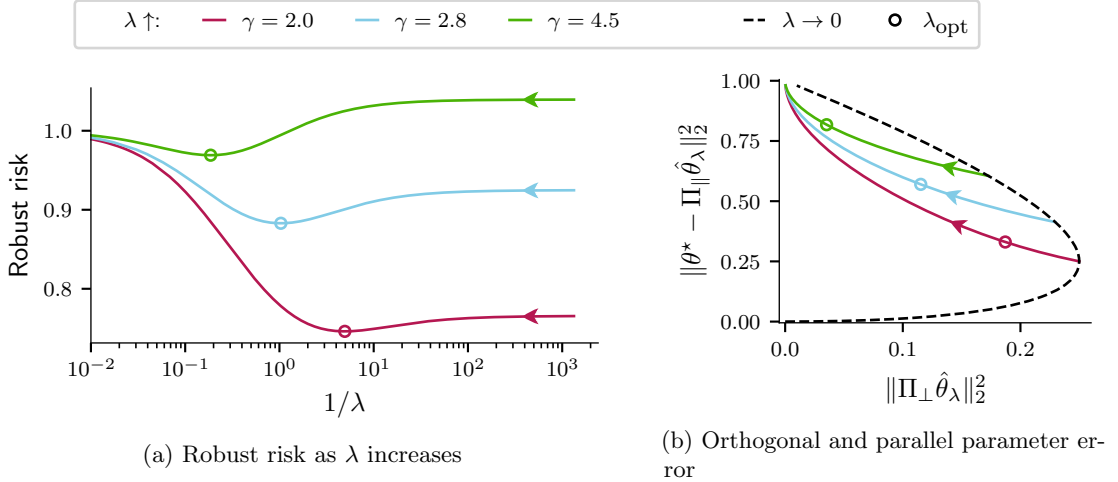


Figure 3: Theoretical curves depicting the robust risk with  $\epsilon = 0.4$  (a) and decomposed terms (b) as  $\lambda$  increases (arrow direction) for different choices of the overparameterization ratio  $d/n \rightarrow \gamma$ . In (b) we observe that for large  $\gamma > 1$ , as  $\lambda$  increases, the orthogonal error  $\|\Pi_{\perp} \hat{\theta}_{\lambda}\|_2$  decreases whereas the parallel error  $\|\theta^* - \Pi_{\parallel} \hat{\theta}_{\lambda}\|_2$  increases. For  $\epsilon > 0$ , the optimal  $\lambda$  is large enough to prevent interpolation.

decomposition into Equation (2) yields the following closed-form expression of the robust risk which now involves the parallel error  $\|\theta^* - \Pi_{\parallel} \hat{\theta}_{\lambda}\|_2^2$  and the orthogonal error  $\|\Pi_{\perp} \hat{\theta}_{\lambda}\|_2^2$ :

$$\mathbf{R}_{\epsilon}(\hat{\theta}_{\lambda}) = \|\theta^* - \Pi_{\parallel} \hat{\theta}_{\lambda}\|_2^2 + (1 + \epsilon^2) \|\Pi_{\perp} \hat{\theta}_{\lambda}\|_2^2 + \sqrt{\frac{8\epsilon^2}{\pi} \|\Pi_{\perp} \hat{\theta}_{\lambda}\|_2^2 (\|\theta^* - \Pi_{\parallel} \hat{\theta}_{\lambda}\|_2^2 + \|\Pi_{\perp} \hat{\theta}_{\lambda}\|_2^2)}. \quad (6)$$

We provide the proof in Appendix A.1.

Figure 3b shows that, as  $\lambda$  increases, the orthogonal error decreases faster than the parallel error increases. Since, by Equation (6), the orthogonal error is weighted more heavily for large enough perturbation strengths  $\epsilon$ , some nonzero ridge coefficient yields the best trade-off. On the other hand, the standard risk with  $\epsilon = 0$  weighs both errors equally, resulting in an optimum at  $\lambda \rightarrow 0$ .

## 4 Max- $\ell_2$ -margin interpolation in robust linear classification

Unlike linear regression, adversarially trained binary logistic regression classifiers may still interpolate the training data, resulting in *robust* max- $\ell_2$ -margin interpolators as  $\lambda \rightarrow 0$ . Hence, in this section we train and evaluate classifiers with  $\ell_{\infty}$ -perturbation sets  $\mathcal{U}_{\infty}(\epsilon)$ , a standard choice in the experimental and theoretical classification literature [19, 24, 42, 47], but also discuss  $\ell_2$ -perturbations in Appendix D.3 for completeness. Our theoretical results show that the robust max- $\ell_2$ -margin interpolator with  $\lambda \rightarrow 0$  has a worse robust risk than a regularized predictor with  $\lambda > 0$ .

### 4.1 Interpolating and regularized estimator

As discussed in Section 3, a common method to obtain robust estimators is to use adversarial training. However, for linear regression, adversarial training either renders interpolating estimators infeasible, or requires oracle knowledge of the ground truth. In contrast, for linear classification, interpolation is easier to achieve – it only requires the sign of  $\langle x_i, \theta \rangle$  to be the same as the label  $y_i$  for all  $i$ . In particular, when the data is sufficiently high dimensional, it is possible to find an interpolator of the adversarially perturbed training set.

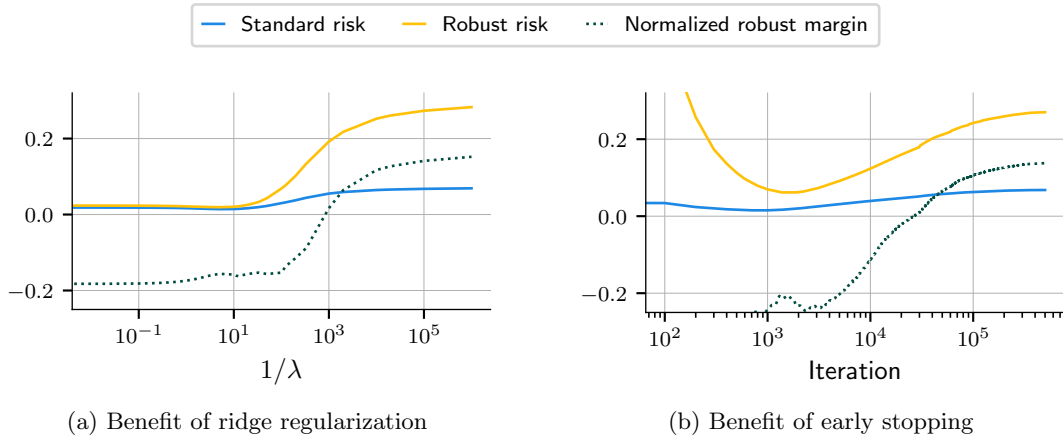


Figure 4: Normalized robust margins and risks of empirical simulations using  $\epsilon = 0.1$  and  $d/n = 8$ , with respect to (a) increasing  $1/\lambda$  and (b) gradient descent iterations when minimizing Equation (7) using  $\lambda = 0$ . Both ridge regularization and early stopping yield superior robust and standard risks. Each experiment uses  $n = 10^3$  and inconsistent  $\ell_\infty$ -perturbations for training. See Appendix B for more details.

We study the robust ridge-regularized logistic regression estimator with penalty weight  $\lambda > 0$ ,

$$\hat{\theta}_\lambda := \arg \min_{\theta} \frac{1}{n} \sum_{i=1}^n \max_{\delta \in \mathcal{U}_\infty(\epsilon)} \log(1 + e^{-(\theta, x_i + \delta)y_i}) + \lambda \|\theta\|_2^2. \quad (7)$$

In the limit  $\lambda \rightarrow 0$  the results in [44] imply that the robust ridge-regularized logistic regression estimator from Equation (7) directionally aligns with the robust max- $\ell_2$ -margin interpolator:<sup>2</sup>

$$\hat{\theta}_0 := \arg \min_{\theta} \|\theta\|_2 \quad \text{such that} \quad \min_{\delta \in \mathcal{U}_\infty(\epsilon)} y_i \langle \theta, x_i + \delta \rangle \geq 1 \text{ for all } i. \quad (8)$$

We say that the data is *robustly separable* if the robust max- $\ell_2$ -margin interpolator exists.

The robust max- $\ell_2$ -margin solution is an interpolating estimator of particular importance since it directionally aligns with the estimator found by gradient descent [31]. Since the robust accuracy (i.e., the robust risk defined using the 0-1 loss) is independent of the norm of the estimator, we simply refer to the robust max- $\ell_2$ -margin solution as the normalized vector  $\frac{\hat{\theta}_0}{\|\hat{\theta}_0\|_2}$ .

In this paper, we study two choices for the set of training perturbations  $\mathcal{U}_\infty(\epsilon)$ :

$$\text{inconsistent perturbations} \quad \mathcal{U}_\infty(\epsilon) = \{\delta \in \mathbb{R}^d : \|\delta\|_\infty \leq \epsilon\} \quad (9)$$

$$\text{consistent perturbations} \quad \mathcal{U}_\infty(\epsilon) = \{\delta \in \mathbb{R}^d : \|\delta\|_\infty \leq \epsilon, \langle \delta, \theta^* \rangle = 0\} \quad (10)$$

Adversarial training with respect to inconsistent perturbations (9) is a popular choice in the literature to improve the robust risk (e.g. [19, 24]). However, perturbed samples may cross the true decision boundary, and hence, inconsistent perturbations effectively introduce noise during the training procedure. In particular, in the data model with noiseless observations that we introduce in Section 4.2, the ground truth function misclassifies approximately 8% of the labels when perturbing the training data with inconsistent perturbations of size  $\epsilon = 0.1$ .

As mentioned in the introduction, in this paper we are interested in verifying whether regularization can be beneficial in high dimensions even in the absence of noise. Therefore, in the sequel we study the impact of both inconsistent (9) and consistent (10) perturbations on robust overfitting.

<sup>2</sup>While [44] only proves the result for  $\epsilon = 0$ , it is straightforward to extend it to the general case where  $\epsilon \geq 0$ .



## 4.2 Robust overfitting in noiseless linear classification

We now show empirically that regularization helps to improve the robust and standard risks when training with noiseless data and derive precise asymptotic predictions for both risks. Throughout this subsection we assume deterministic, and hence, noiseless training labels, i.e.,  $y_i = \text{sgn}\langle x_i, \theta^* \rangle$ . Furthermore, as we discuss in Section 4.3, the inductive bias of the  $\ell_\infty$ -robust logistic loss encourages sparse solutions. Since we are primarily interested in learning ground truth functions that match the implicit bias of the estimator, we assume the sparse ground truth  $\theta^* = (1, 0, \dots, 0)^T$ .

We first show robust overfitting experimentally on noiseless data when training with inconsistent perturbations and subsequently demonstrate that overfitting persists even if the training procedure is completely noiseless (i.e., using consistent training perturbations). Finally, we provide theoretical evidence for our observations in the high-dimensional asymptotic limit.

**Training with inconsistent adversarial perturbations** Figure 4a illustrates the *robust margin*  $\min_i \min_{\delta \in \mathcal{U}_\infty(\epsilon)} \frac{1}{\|\theta\|_2} y_i \langle \theta, x_i + \delta \rangle$  as well as the standard and robust risks of the estimator  $\hat{\theta}_\lambda$  trained using inconsistent adversarial perturbations on a synthetic data set with fixed overparameterization ratio  $d/n = 8$ . We observe that decreasing the ridge coefficient well beyond the point where the minimizer of the robust logistic loss (7) reaches 100% robust training accuracy (i.e., the robust margin becomes positive) substantially hurts generalization.

In addition to varying the ridge coefficient  $\lambda$ , we notice that the same trends as for  $\lambda \rightarrow 0$  also occur for the gradient descent optimization path as the number of iterations  $t$  goes to infinity. Figure 4b indicates that, similarly to ridge regularization, early stopping also avoids the robust max- $\ell_2$ -margin solution that is obtained for  $t \rightarrow \infty$  and yields an estimator with significantly lower standard and robust risks.

**Training with consistent adversarial perturbations** As discussed in Section 4.1, even for noiseless training data, inconsistent perturbations can induce noise during the training procedure. Hence, one could hypothesize that the noise induced by the inconsistent perturbations causes the overfitting observed in Figure 4. To contradict this hypothesis, we also study adversarial training with consistent perturbations. By definition, consistent perturbations do not cross the true decision boundary and hence leave the training data entirely noiseless.

Figure 5a shows that the adversarially trained estimators (7),(8) with consistent and inconsistent perturbations yield comparable robust risks. Moreover, robust overfitting occurs in both situations, as the risk is higher for the interpolating estimator  $\lambda \rightarrow 0$  compared to an optimal  $\lambda > 0$ . Hence, our observations demonstrate that robust overfitting persists even if training with consistent perturbations in an entirely noiseless setting. This observation is counter intuitive since, according to classical wisdom, we would expect ridge regularization to only benefit in noisy settings where the estimator suffers from a high variance.

We now prove this phenomenon using the next theorem. In particular, similar to Theorem 3.1 for linear regression, we show that robust overfitting occurs in the high-dimensional asymptotic regime where  $d/n \rightarrow \gamma$  as  $d, n \rightarrow \infty$ . We state an informal version of the theorem in the main text and refer to Appendix F for the precise statement. The proof is inspired by the works [24, 46] and uses the Convex Gaussian Minimax Theorem (CGMT) [20, 51].

**Theorem 4.1 (Informal).** *Assume that  $\epsilon = \epsilon_0/\sqrt{d}$  for some constant  $\epsilon_0$  and  $\theta^* = (1, 0, \dots, 0)^T$ . Then, the robust and standard risks of the regularized estimator  $\hat{\theta}_\lambda$  (7) ( $\lambda > 0$ ) and of the robust max- $\ell_2$ -margin interpolator (8) ( $\lambda \rightarrow 0$ ) with inconsistent (9) or consistent (10) adversarial  $\ell_\infty$ -perturbations converge in probability as  $d, n \rightarrow \infty$ ,  $d/n \rightarrow \gamma$  to:*

$$\mathbf{R}(\hat{\theta}_\lambda) \rightarrow \frac{1}{\pi} \arccos\left(\frac{\nu_\parallel^*}{\nu^*}\right) \quad \text{and} \quad \mathbf{R}_\epsilon(\hat{\theta}_\lambda) \rightarrow \mathbf{R}(\hat{\theta}_\lambda) + \frac{1}{2} \text{erf}\left(\frac{\epsilon_0 \delta^*}{\sqrt{2} \nu^*}\right) + I\left(\frac{\epsilon_0 \delta^*}{\nu^*}, \frac{\nu_\parallel^*}{\nu^*}\right)$$

We denote by  $\text{erf}(\cdot)$  the error function,

$$I(t, u) := \int_0^t \frac{1}{\sqrt{2\pi}} \exp\left(-\frac{x^2}{2}\right) \text{erf}\left(\frac{xu}{\sqrt{2(1-u^2)}}\right) dx,$$



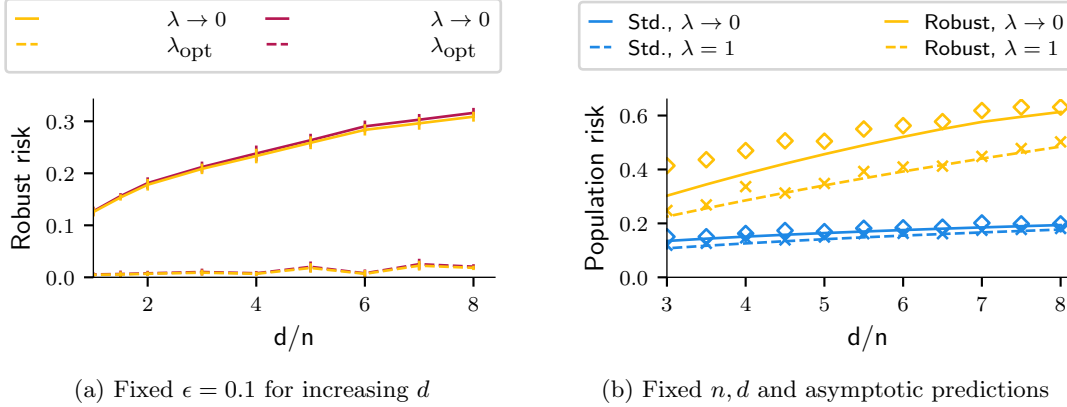


Figure 5: (a) Comparison of consistent and inconsistent  $\ell_\infty$ -perturbations for adversarial logistic regression with respect to the degree of overparameterization  $d/n$ , using  $\epsilon = 0.1$  for both training and evaluation. Note that both estimators behave very similarly, implying that the effect of inconsistency is negligible for small  $\epsilon$ . (b) Robust and standard risks of the robust max- $\ell_2$ -margin interpolator ( $\lambda \rightarrow 0$ ) and robust ridge estimate ( $\lambda = 1$ ) with consistent perturbations (10) using  $\epsilon = 0.05$  as a function of the overparameterization ratio  $d/n$  for simulations (markers) and asymptotic theoretical predictions from Theorem 4.1 (lines). We note that, for small values of  $\gamma$ , solving the optimization problem that gives the theoretical predictions becomes numerically unstable. All simulations use  $n = 10^3$  samples from our data model; see Appendix B for further experimental details.

and use the notation  $\nu^* = \sqrt{(\nu_\perp^*)^2 + (\nu_\parallel^*)^2}$ , where  $\nu_\perp^*, \nu_\parallel^*, \delta^*$  are the unique solution of a scalar optimization problem specified in Appendix F that depends on  $\theta^*, \gamma, \epsilon_0$  and  $\lambda$ .

Since the theoretical expressions are hard to interpret, we visualize the asymptotic values of the standard and robust risks from Theorem 4.1 in Figure 5b by solving the scalar optimization problem specified in Appendix F. We observe that Theorem 4.1 indeed predicts the benefits of regularization for robust logistic regression and that simulations using finite values of  $d$  and  $n$  follow the asymptotic trend. We describe the full empirical setup in Appendix B.

### 4.3 Intuitive explanation and discussion

Even though we explicitly derive the precise asymptotic expressions of the standard and robust risks in Theorem 4.1 that predict the benefits of regularization for generalization, it is difficult to extract intuitive explanations for this phenomenon directly from the proof. We conjecture that a non-zero ridge penalty induces a more sparse  $\hat{\theta}_\lambda$  (i.e., with a smaller  $\ell_1/\ell_2$ -norm ratio) than the robust max- $\ell_2$ -margin solution  $\hat{\theta}_0$  and use simulations to support our claim. Since the  $\ell_\infty$ -adversarially robust risk penalizes dense solutions with large ratio of the  $\ell_1/\ell_2$ -norms (see Lemma A.2 in Appendix A.2), we expect more sparse estimators to have a lower robust risk. Indeed, Figure 6a shows that the  $\ell_1/\ell_2$ -norm ratio strongly correlates with the robust risk of the estimator.

We begin by noting that, due to Lagrangian duality, minimizing the ridge-penalized loss (7) corresponds to minimizing the unregularized loss constrained to the set of estimators  $\theta$  with a bounded  $\ell_2$ -norm. This norm decreases as the ridge coefficient  $\lambda$  increases. In what follows, we provide intuition on the effect of the ridge penalty  $\lambda$  on the sparsity of the estimator  $\hat{\theta}_\lambda$ .

**Large  $\lambda$  inducing a small  $\ell_2$ -norm** We first analyze the regularized estimator  $\hat{\theta}_\lambda$  for large  $\lambda$  that constrains solutions to have small  $\ell_2$ -norm. We can therefore use Taylor’s theorem and the closed-form expression of adversarial perturbations (see Lemma A.2 in Appendix A.2) to approximate

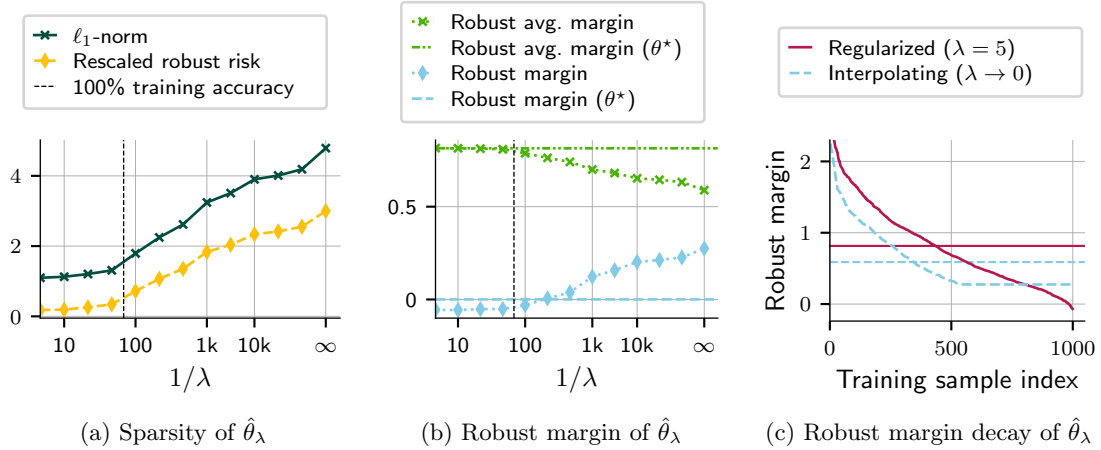


Figure 6: (a) The  $\ell_1$ -norm and the rescaled (by a factor of 10) robust risk of the estimator with respect to  $1/\lambda$ . (b) The robust average margin contrasted to the robust margin as a function of  $1/\lambda$ . The horizontal lines denote the corresponding values for  $\theta^*$ . (c) The ordered sample-wise robust margins  $y_i \langle x_i, \theta \rangle - \epsilon \|\Pi_{\perp} \theta\|_1$  when interpolating and regularizing. For larger  $\lambda$ , the robust (*minimum*) margin decreases while the robust average margin (horizontal lines) increases. We normalize the estimators, i.e.,  $\|\hat{\theta}_{\lambda}\|_2 = 1$ , for all curves presented in the plots; see Appendix B for further experimental details.

the unregularized robust loss from Equation (7) as follows:

$$\frac{1}{n} \sum_{i=1}^n \log(1 + e^{-y_i \langle \theta, x_i \rangle + \epsilon \|\Pi_{\perp} \theta\|_1}) \approx \frac{1}{n} \sum_{i=1}^n -y_i \langle x_i, \theta \rangle + \epsilon \|\Pi_{\perp} \theta\|_1. \quad (11)$$

As a consequence, the minimizer  $\hat{\theta}_{\lambda}$  should result in a large *robust average margin* solution, that is, a solution with large  $\frac{1}{n} \sum_{i=1}^n \frac{1}{\|\theta\|_2} (y_i \langle x_i, \theta \rangle - \epsilon \|\Pi_{\perp} \theta\|_1)$ . Indeed, we observe this using simulations for finite  $d, n$  in Figures 6b and 6c. In particular, the objective in Equation (11) leads to a trade-off between the sparsity of the estimator (via its convex surrogate, the  $\ell_1$ -norm) and an *average* of the sample-wise margins  $y_i \langle x_i, \theta \rangle$ . We note that such estimators have been well studied in the literature and are known to achieve good performance in recovering sparse ground truths [5, 17, 39].

**Small  $\lambda$  inducing a large  $\ell_2$ -norm** In contrast, a small ridge coefficient  $\lambda$  leads to estimators  $\hat{\theta}_{\lambda}$  with large  $\ell_2$ -norms. In this case, the estimator approaches a large *robust (minimum) margin* solution, i.e., a solution with large  $\min_i \frac{1}{\|\theta\|_2} (y_i \langle x_i, \theta \rangle - \epsilon \|\Pi_{\perp} \theta\|_1)$  which is maximized by the robust max- $\ell_2$ -margin interpolator (8). As a consequence, this leads to a trade-off between estimator sparsity and the robust minimum margin  $\min_i \frac{1}{\|\theta\|_2} y_i \langle x_i, \theta \rangle$ . Due to the high dimensionality of the input data, the training samples  $x_i$  are approximately orthogonal. Thus, to achieve a non-vanishing robust margin, estimators are forced to trade-off sparsity with *all* sample-wise margins instead of just the average. We reveal this trade-off in Figures 6a and 6b where the increase in  $\ell_1/\ell_2$ -norm ratios corresponds to a decrease in the robust average margin and an increase in the robust margin.

Finally, we observe that the *sparse* ground truth is characterized by a large robust average margin (horizontal dotted line in Figure 6b) and a small (minimum) robust margin (horizontal dashed line). Therefore, we expect that the solution that is sparser and which satisfies the same properties for the robust margin as the ground truth  $\theta^*$ , will achieve lower robust and standard risks. Indeed, our findings indicate that the regularized estimator  $\hat{\theta}_{\lambda}$  for large  $\lambda$  aligns better with  $\theta^*$ , compared to the solution obtained for a small  $\lambda$ , and hence justify the better performance of ridge-regularized predictors.

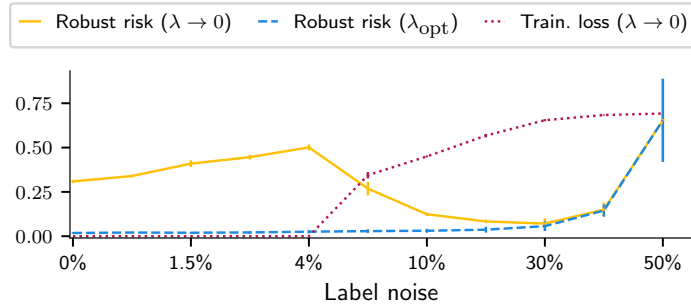


Figure 7: Training loss and robust risks with respect to increasing training label noise for  $\epsilon = 0.1$ ,  $d = 8 \times 10^3$  and  $n = 10^3$ . We observe for unregularized estimators ( $\lambda \rightarrow 0$ ) that, counterintuitively, moderate amounts of label noise decrease the robust risk by avoiding the robust max- $\ell_2$ -margin solution. While this might spuriously imply that injecting label noise increases robustness, estimators with optimal ridge parameter  $\lambda_{\text{opt}}$  still outperform their unregularized counterparts in terms of robust risk. Since the setting is noisy, we average the risks over five independent dataset draws and indicate standard deviations via error bars.

#### 4.4 Benefits of an unorthodox way to avoid the robust max- $\ell_2$ -margin interpolator

In the previous subsections we focused on robustly separable data and studied the generalization performance of regularized estimators that do not maximize the robust margin. Another way to avoid the robust max- $\ell_2$ -margin solution is to introduce enough label noise in the training data. We now show that, unexpectedly, this unorthodox way to avoid the robust max-margin solution can also yield an estimator with better robust generalization than the robust max- $\ell_2$ -margin solution of the corresponding noiseless problem.

Specifically, in our experiments we introduce noise by flipping the labels of a fixed fraction of the training data. Figure 7 shows the robust and standard risks together with the training loss of the estimator  $\hat{\theta}_\lambda$  from Equation (7) trained with consistent perturbations for  $\lambda \rightarrow 0$  with varying fractions of flipped labels. For low noise levels, the data is robustly separable and the training loss vanishes at convergence, yielding the robust max- $\ell_2$ -margin solution in Equation (8). For high enough noise levels, the constraints in Equation (8) become infeasible and the training loss of the resulting estimator starts to increase. As discussed in Subsection 4.3, this estimator has a better implicit bias than the robust max- $\ell_2$ -margin interpolator and hence achieves a lower robust risk.

Even though it is well known that introducing covariate noise can induce implicit regularization [8], our observations show that in contrast to common intuition, the robust risk also decreases when introducing wrong labels in the training loss. In parallel to our work, the paper [30] shows that training with corrupted labels can be beneficial for the standard risk.

However, we emphasize here that we do not advocate in favor of artificial label noise as a means to obtain more robust classifiers. In particular, even if the data is not robustly separable, the estimator with optimal ridge parameter  $\lambda_{\text{opt}}$  in Figure 7 still always outperforms the unregularized solution.

Finally, we remark that a similar effect can also be observed when training with inconsistent perturbations with large perturbation norm  $\epsilon$ . We refer to Appendix D.1 for further discussion.

## 5 Related work

**Understanding robust overfitting** The current literature attempting to explain robust overfitting [42] primarily focuses on the effect of noise and on the smoothness of decision boundaries learned by neural networks trained to convergence [16, 47, 53]. A slightly different line of work [45] shows that overparameterized models require regularization in order to achieve good classification accuracy on all subpopulations. However, a theoretical understanding of the role of regularization is still missing.

**Theory for adversarial robustness of linear models** Recent works [24, 25] provide a precise description of the robust risks for logistic and linear regression when trained with adversarial attacks based on the Convex Gaussian Minimax Theorem [20, 51]. The analysis focuses on inconsistent attacks for both training and evaluation. For linear regression, the authors observe that adversarial training with  $\ell_2$ -perturbations mitigates the peak in the double descent curve around  $d = n$  and hence acts similarly to ridge regularization as explicitly studied in [23]. Several other works focus on the role of gradient descent in robust logistic regression. In particular, [56] proves that early stopping yields robust adversarially-trained linear classifiers even in the presence of noise. Furthermore, the results of [31] show that gradient descent on robustly separable data converges to the robust max- $\ell_2$ -margin estimator (8).

## 6 Conclusion and future work

In this work, we show that overparameterized linear models can overfit with respect to the robust risk even when there is no noise in the training data. Our results challenge the modern narrative that interpolating overparameterized models yield good performance without explicit regularization and motivate the use of ridge regularization and early stopping for improved robust generalization. Perhaps surprisingly, we further observe that ridge regularization enhances the bias of logistic regression trained with adversarial  $\ell_\infty$ -attacks towards sparser solutions, indicating that the impact of explicit regularization may go well beyond variance reduction.

**Future work** Our simulations indicate that early stopping yields similar benefits as ridge regularization in noiseless settings. However, we leave a formal proof for future work. Furthermore, the double descent phenomenon has been proven for the standard risk on a broad variety of data distributions and even for non-linear models such as random feature regression. It is still unclear how our results translate to these settings. In particular, our theoretical analysis heavily makes use of the closed-form solution of the adversarial attacks, and hence, cannot be applied to non-linear models in a straightforward way.

## Acknowledgments

K. D. is supported by the ETH AI Center and the ETH Foundations of Data Science. R. H. is supported by the IAS at TUM, the DFG (German Research Foundation), and by the NSF under award IIS-1816986.

## References

- [1] A. Ali, J. Z. Kolter, and R. J. Tibshirani. A continuous-time view of early stopping for least squares regression. In *Proceedings of the International Conference on Artificial Intelligence and Statistics (AISTATS)*, volume 89, pages 1370–1378, 2019.
- [2] A. Ali, E. Dobriban, and R. Tibshirani. The implicit regularization of stochastic gradient flow for least squares. In *Proceedings of the International Conference on Machine Learning (ICML)*, volume 119, pages 233–244, 2020.
- [3] Z. Bai and J. W. Silverstein. *Spectral analysis of large dimensional random matrices*, volume 20. Springer, 2010.
- [4] Z. D. Bai and Y. Q. Yin. Limit of the smallest eigenvalue of a large dimensional sample covariance matrix. *The Annals of Probability*, 21:1275–1294, 1993.
- [5] P. Bartlett, Y. Freund, W. S. Lee, and R. E. Schapire. Boosting the margin: A new explanation for the effectiveness of voting methods. *The Annals of Statistics*, 26:1651 – 1686, 1998.
- [6] P. L. Bartlett, P. M. Long, G. Lugosi, and A. Tsigler. Benign overfitting in linear regression. In *Proceedings of the National Academy of Sciences*, volume 117, pages 30063–30070, 2020.
- [7] M. Belkin, D. Hsu, S. Ma, and S. Mandal. Reconciling modern machine-learning practice and the classical bias–variance trade-off. In *Proceedings of the National Academy of Sciences*, volume 116, pages 15849–15854, 2019.
- [8] C. Bishop. Training with noise is equivalent to Tikhonov regularization. *Neural Computation*, 7: 108–116, 1995.
- [9] P. Bühlmann and S. Van De Geer. *Statistics for high-dimensional data: Methods, theory and applications*. Springer Science & Business Media, 2011.
- [10] P. Bühlmann et al. Invariance, causality and robustness. *Statistical Science*, 35:404–426, 2020.
- [11] Y. Chen and P. Bühlmann. Domain adaptation under structural causal models. *arXiv preprint arXiv:2010.15764*, 2020.
- [12] L. Chizat and F. Bach. On the global convergence of gradient descent for over-parameterized models using optimal transport. In *Advances in Neural Information Processing Systems (NeurIPS)*, volume 31, 2018.
- [13] L. Chizat and F. Bach. Implicit bias of gradient descent for wide two-layer neural networks trained with the logistic loss. In *Proceedings of the Conference on Learning Theory (COLT)*, volume 125, pages 1305–1338, 2020.
- [14] Z. Deng, A. Kammoun, and C. Thrampoulidis. A model of double descent for high-dimensional binary linear classification. In *Information and Inference: A Journal of the IMA*, volume 4, 2021.
- [15] E. Dobriban and S. Wager. High-dimensional asymptotics of prediction: Ridge regression and classification. *The Annals of Statistics*, 46:247 – 279, 2018.
- [16] C. Dong, L. Liu, and J. Shang. Data profiling for adversarial training: On the ruin of problematic data. *arXiv preprint arXiv:2102.07437*, 2021.
- [17] W. Gao and Z.-H. Zhou. On the doubt about margin explanation of boosting. *Artificial Intelligence*, 203:1–18, 2013.
- [18] B. Ghorbani, S. Mei, T. Misiakiewicz, and A. Montanari. Linearized two-layers neural networks in high dimension. *The Annals of Statistics*, 49:1029 – 1054, 2021.

- [19] I. Goodfellow, J. Shlens, and C. Szegedy. Explaining and harnessing adversarial examples. In *Proceedings of the International Conference on Learning Representations (ICLR)*, 2015.
- [20] Y. Gordon. On Milman’s inequality and random subspaces which escape through a mesh in  $\mathbb{R}^n$ . In *Geometric aspects of functional analysis*, pages 84–106. 1988.
- [21] P. Grother, G. Quinn, and P. Phillips. Report on the evaluation of 2D still-image face recognition algorithms, 2010.
- [22] S. Gunasekar, J. D. Lee, D. Soudry, and N. Srebro. Implicit bias of gradient descent on linear convolutional networks. In *Advances in Neural Information Processing Systems (NeurIPS)*, volume 31, 2018.
- [23] T. Hastie, A. Montanari, S. Rosset, and R. J. Tibshirani. Surprises in high-dimensional ridgeless least squares interpolation. *arXiv preprint arXiv:1903.08560*, 2019.
- [24] A. Javanmard and M. Soltanolkotabi. Precise statistical analysis of classification accuracies for adversarial training. *arXiv preprint arXiv:2010.11213*, 2020.
- [25] A. Javanmard, M. Soltanolkotabi, and H. Hassani. Precise tradeoffs in adversarial training for linear regression. In *Proceedings of the Conference on Learning Theory (COLT)*, volume 125, pages 2034–2078, 2020.
- [26] Z. Ji and M. Telgarsky. Gradient descent aligns the layers of deep linear networks. In *Proceedings of the International Conference on Learning Representations (ICLR)*, 2019.
- [27] Z. Ji and M. Telgarsky. The implicit bias of gradient descent on nonseparable data. In *Proceedings of the Conference on Learning Theory (COLT)*, volume 99, pages 1772–1798, 2019.
- [28] A. Knowles and J. Yin. Anisotropic local laws for random matrices. *Probability Theory and Related Fields*, 169:257–352, 2014.
- [29] D. Kobak, J. Lomond, and B. Sanchez. The optimal ridge penalty for real-world high-dimensional data can be zero or negative due to the implicit ridge regularization. *Journal of Machine Learning Research*, 21:1–16, 2020.
- [30] Y. Lee and R. F. Barber. Binary classification with corrupted labels. *arXiv preprint arXiv:2106.09136*, 2021.
- [31] Y. Li, E. X. Fang, H. Xu, and T. Zhao. Implicit bias of gradient descent based adversarial training on separable data. In *Proceedings of the International Conference on Learning Representations (ICLR)*, 2020.
- [32] K. Lyu and J. Li. Gradient descent maximizes the margin of homogeneous neural networks. In *Proceedings of the International Conference on Learning Representations (ICLR)*, 2020.
- [33] S. Mei and A. Montanari. The generalization error of random features regression: Precise asymptotics and double descent curve. *arXiv preprint arXiv:1908.05355*, 2019.
- [34] V. Muthukumar, A. Narang, V. Subramanian, M. Belkin, D. Hsu, and A. Sahai. Classification vs regression in overparameterized regimes: Does the loss function matter? *arXiv preprint arXiv:2005.08054*, 2020.
- [35] V. Muthukumar, K. Vodrahalli, V. Subramanian, and A. Sahai. Harmless interpolation of noisy data in regression. *IEEE Journal on Selected Areas in Information Theory*, 1:67–83, 2020.
- [36] P. Nakkiran, G. Kaplun, Y. Bansal, T. Yang, B. Barak, and I. Sutskever. Deep double descent: Where bigger models and more data hurt. In *Proceedings of the International Conference on Learning Representations (ICLR)*, 2020.

- [37] P. Nakkiran, P. Venkat, S. M. Kakade, and T. Ma. Optimal regularization can mitigate double descent. In *Proceedings of the International Conference on Learning Representations (ICLR)*, 2021.
- [38] P. Patil, Y. Wei, A. Rinaldo, and R. Tibshirani. Uniform consistency of cross-validation estimators for high-dimensional ridge regression. In *Proceedings of the International Conference on Artificial Intelligence and Statistics (AISTATS)*, volume 130, pages 3178–3186, 2021.
- [39] Y. Plan and R. Vershynin. Robust 1-bit compressed sensing and sparse logistic regression: A convex programming approach. In *IEEE Transactions on Information Theory*, volume 59, 2012.
- [40] J. Quionero-Candela, M. Sugiyama, A. Schwaighofer, and N. D. Lawrence. *Dataset Shift in Machine Learning*. The MIT Press, 2009.
- [41] A. Raghunathan, S. M. Xie, F. Yang, J. Duchi, and P. Liang. Understanding and mitigating the tradeoff between robustness and accuracy. In *Proceedings of the International Conference on Machine Learning (ICML)*, volume 119, pages 11146–11156, 2020.
- [42] L. Rice, E. Wong, and Z. Kolter. Overfitting in adversarially robust deep learning. In *Proceedings of the International Conference on Machine Learning (ICML)*, volume 119, pages 8093–8104, 2020.
- [43] D. Richards, J. Mourtada, and L. Rosasco. Asymptotics of ridge (less) regression under general source condition. In *Proceedings of the International Conference on Artificial Intelligence and Statistics (AISTATS)*, volume 130, pages 3889–3897, 2021.
- [44] S. Rosset, J. Zhu, and T. Hastie. Margin maximizing loss functions. In *Advances in Neural Information Processing Systems (NeurIPS)*, volume 16, 2004.
- [45] S. Sagawa, P. W. Koh, T. B. Hashimoto, and P. Liang. Distributionally robust neural networks. In *Proceedings of the International Conference on Learning Representations (ICLR)*, 2020.
- [46] F. Salehi, E. Abbasi, and B. Hassibi. The impact of regularization on high-dimensional logistic regression. In *Advances in Neural Information Processing Systems (NeurIPS)*, volume 32, 2019.
- [47] A. Sanyal, P. K. Dokania, V. Kanade, and P. Torr. How benign is benign overfitting? In *Proceedings of the International Conference on Learning Representations (ICLR)*, 2021.
- [48] A. Sinha, H. Namkoong, and J. Duchi. Certifying some distributional robustness with principled adversarial training. In *Proceedings of the International Conference on Learning Representations (ICLR)*, 2018.
- [49] D. Soudry, E. Hoffer, M. S. Nacson, S. Gunasekar, and N. Srebro. The implicit bias of gradient descent on separable data. *Journal of Machine Learning Research*, 19:1–57, 2018.
- [50] P. Sur and E. J. Candès. A modern maximum-likelihood theory for high-dimensional logistic regression. In *Proceedings of the National Academy of Sciences*, volume 116, pages 14516–14525, 2019.
- [51] C. Thrampoulidis, S. Oymak, and B. Hassibi. Regularized linear regression: A precise analysis of the estimation error. In *Proceedings of the Conference on Learning Theory (COLT)*, volume 40, pages 1683–1709, 2015.
- [52] M. Wainwright. *High-Dimensional Statistics: A Non-Asymptotic Viewpoint*. Cambridge University Press, 2019.
- [53] B. Wu, J. Chen, D. Cai, X. He, and Q. Gu. Do wider neural networks really help adversarial robustness? *arXiv preprint arXiv:2010.01279*, 2020.



- [54] D. Wu and J. Xu. On the optimal weighted  $\ell_2$  regularization in overparameterized linear regression. *arXiv preprint arXiv:2006.05800*, 2020.
- [55] B. Zadrozny. Learning and evaluating classifiers under sample selection bias. In *Proceedings of the International Conference on Machine Learning (ICML)*, 2004.
- [56] D. Zou, S. Frei, and Q. Gu. Provable robustness of adversarial training for learning halfspaces with noise. In *Proceedings of the International Conference on Machine Learning (ICML)*, volume 139, pages 13002–13011, 2021.

## A Closed form expressions for the robust risks

In Section A.1 and A.2 we derive closed-form expressions of the standard and robust risks from Equations (1),(2) for the settings studied in Section 3.4. We use those expressions repeatedly in our proofs. Furthermore, Section A.3 discusses that the robust risk (2) upper-bounds the worst case risk under distributional mean shifts.

### A.1 Closed-form of robust risk for regression

The following lemma provides a closed-form expression of the robust risk for the linear regression setting studied in Section 3. A similar result for inconsistent attacks has already been shown before (Lemma 3.1. in [25]); we only include the proof for completeness.

**Lemma A.1.** *Assume that  $\mathbb{P}_X$  is the isotropic Gaussian distribution. Then, for the square loss, the robust risk (2) with respect to  $\ell_2$ -perturbations is given by*

$$\mathbf{R}_\epsilon(\theta) = \|\theta^* - \theta\|_2^2 + 2\epsilon\sqrt{2/\pi}\|\Pi_\perp\theta\|_2\|\theta^* - \theta\|_2 + \epsilon^2\|\Pi_\perp\theta\|_2^2. \quad (12)$$

*Proof.* Define  $\tilde{y}_i = y_i - \langle x_i, \theta \rangle$ , and note that using similar arguments as in Section 6.2. [25]

$$\begin{aligned} \max_{\delta_i \in \mathcal{U}_2(\epsilon)} (\tilde{y}_i - \langle \delta_i, \theta \rangle)^2 &= \left( \max_{\delta_i \in \mathcal{U}_2(\epsilon)} |\tilde{y}_i - \langle \delta_i, \theta \rangle| \right)^2 \\ &= (|\tilde{y}_i| + \max_{\|\delta_i\|_2 \leq \epsilon, \delta_i \perp \theta^*} |\langle \delta_i, \theta \rangle|)^2 \\ &= (|\tilde{y}_i| + \epsilon\|\Pi_\perp\theta\|_2)^2. \end{aligned}$$

With this characterization, we can derive a convenient expression for the robust risk:

$$\begin{aligned} \mathbf{R}_\epsilon(\theta) &= \mathbb{E}_X (|\langle X, \theta^* - \theta \rangle| + \epsilon\|\Pi_\perp\theta\|_2)^2 \\ &= \mathbb{E}_X (\langle X, \theta^* - \theta \rangle)^2 + 2\epsilon\mathbb{E}_X |\langle X, \theta^* - \theta \rangle| \|\Pi_\perp\theta\|_2 + \epsilon^2\|\Pi_\perp\theta\|_2^2. \end{aligned} \quad (13)$$

Since we assume isotropic Gaussian features, that is  $\mathbb{P}_X = \mathcal{N}(0, I)$ , we can further simplify

$$\mathbf{R}_\epsilon(\theta) = \|\theta - \theta^*\|_2^2 + 2\epsilon\sqrt{2/\pi}\|\Pi_\perp\theta\|_2\|\theta - \theta^*\|_2 + \epsilon^2\|\Pi_\perp\theta\|_2^2$$

which concludes the proof.  $\square$

### A.2 Closed-form of robust risk for classification

Similarly to linear regression, we can express the robust and standard risk for the linear classification model in Section 4 as stated in the following lemma.

**Lemma A.2.** *Assume that  $\mathbb{P}_X$  is the isotropic Gaussian distribution and  $\theta^* = (1, 0, \dots, 0)^\top$ . Then,*

1. *For any non-decreasing loss  $\ell : \mathbb{R} \rightarrow \mathbb{R}$  we have*

$$\max_{\delta_i \in \mathcal{U}_\infty(\epsilon)} \ell(y_i \langle x_i + \delta_i, \theta \rangle) = \ell(y_i \langle x_i, \theta \rangle - \epsilon\|\Pi_\perp\theta\|_1). \quad (14)$$

2. *For the 0-1 loss the robust risk (2) with respect to  $\ell_\infty$ -perturbations is given by*

$$\mathbf{R}_\epsilon(\theta) = \frac{1}{\pi} \arccos \left( \frac{\langle \theta^*, \theta \rangle}{\|\theta\|_2} \right) + \frac{1}{2} \operatorname{erf} \left( \frac{\epsilon\|\Pi_\perp\theta\|_1}{\sqrt{2}\|\theta\|_2} \right) + I \left( \frac{\epsilon\|\Pi_\perp\theta\|_1}{\|\theta\|_2}, \frac{\langle \theta^*, \theta \rangle}{\|\theta\|_2} \right), \quad (15)$$

with

$$I(t, u) := \int_0^t \frac{1}{\sqrt{2\pi}} \exp \left( -\frac{x^2}{2} \right) \Phi \left( \frac{xu}{\sqrt{2}\sqrt{1-u^2}} \right) dx. \quad (16)$$

*Proof.* We first prove Equation (14). Because  $\ell$  is non-increasing, we have

$$\begin{aligned} \max_{\delta_i \in \mathcal{U}_\infty(\epsilon)} \ell(y_i \langle x_i + \delta_i, \theta \rangle) &= \ell\left(\min_{\delta_i \in \mathcal{U}_\infty(\epsilon)} y_i \langle x_i + \delta_i, \theta \rangle\right) \\ &= \ell(y_i \langle x_i, \theta \rangle + \min_{\|\delta_i\|_\infty \leq \epsilon, \delta_i \perp \theta^*} \langle \delta_i, \theta \rangle) \\ &= \ell(y_i \langle x_i, \theta \rangle) - \epsilon \|\Pi_\perp \theta\|_1, \end{aligned}$$

which establishes Equation (14). Note that for the last equation we used that, while minimization over  $\delta$  has no closed-form solution in general, for our choice of  $\theta^* = (1, 0, \dots, 0)$ , we get  $\min_{\|\delta_i\|_\infty \leq \epsilon, \delta_i \perp \theta^*} \langle \delta_i, \theta \rangle = -\epsilon \|\Pi_\perp \theta\|_1$ .

We now prove the second part of the statement. Let  $\mathbb{1}\{E\}$  be the indicator function, which is 1 if the event  $E$  occurs, and 0 otherwise. Since  $\ell(\cdot) = \mathbb{1}_{\leq 0}$  is non-increasing we can use (14) and write

$$\begin{aligned} \mathbf{R}_\epsilon(\theta) &= \mathbb{E}_X \max_{\delta \in \mathcal{U}_\infty(\epsilon)} \mathbb{1}\{\text{sgn}(\langle X, \theta^* \rangle) \langle X + \delta, \theta \rangle \leq 0\} \\ &= \mathbb{E}_X \mathbb{1}\{\text{sgn}(\langle X, \theta^* \rangle) \langle X, \theta \rangle - \epsilon \|\Pi_\perp \theta\|_1 \leq 0\}. \end{aligned}$$

Let  $\widehat{\Pi}_\parallel := \frac{1}{\|\theta\|_2^2} \theta \theta^\top$  be the projection onto the subspace spanned by  $\theta$  and  $\widehat{\Pi}_\perp := I_d - \widehat{\Pi}_\parallel$  the projection onto the orthogonal complement. Since  $X$  is a vector with i.i.d. standard normal distributed entries, we equivalently have

$$\mathbf{R}_\epsilon(\theta) = \mathbb{E}_{Z_1, Z_2} \mathbb{1}\{Z_1 \text{sgn}\left(Z_1 \|\widehat{\Pi}_\parallel \theta^*\|_2 + Z_2 \|\widehat{\Pi}_\perp \theta^*\|_2\right) - \epsilon \frac{\|\Pi_\perp \theta\|_1}{\|\theta\|_2} \leq 0\}, \quad (17)$$

with  $Z_1, Z_2$  two independent standard normal random variables. For brevity of notation, define  $\nu = \epsilon \frac{\|\Pi_\perp \theta\|_1}{\|\theta\|_2}$  and  $b(Z_1, Z_2) = \text{sgn}\left(Z_1 \|\widehat{\Pi}_\parallel \theta^*\|_2 + Z_2 \|\widehat{\Pi}_\perp \theta^*\|_2\right) =: \text{sgn}(\beta^\top Z)$  with  $\beta^\top = (\|\widehat{\Pi}_\parallel \theta^*\|_2, \|\widehat{\Pi}_\perp \theta^*\|_2)$ .

Define the event  $A = \{\text{sgn}\left(Z_1 \|\widehat{\Pi}_\parallel \theta^*\|_2 + Z_2 \|\widehat{\Pi}_\perp \theta^*\|_2\right) - \epsilon \frac{\|\Pi_\perp \theta\|_1}{\|\theta\|_2} \leq 0\}$ . Because  $Z_2$  is symmetric, the distribution of  $Z_1 b(Z_1, Z_2)$  is symmetric, hence we can rewrite the risk

$$\mathbf{R}_\epsilon(\theta) = \underbrace{\mathbb{P}(b(Z_1, Z_2) \leq 0 | Z_1 \geq 0)}_{T_1} + \underbrace{\mathbb{P}(Z_1 \leq \nu, b(Z_1, Z_2) \geq 0 | Z_1 \geq 0)}_{T_2} \quad (18)$$

and derive expression for  $T_1, T_2$  separately.

**Step 1: Proof for  $T_1$**  Note that due to  $\|\theta^*\|_2 = 1$  we have  $\|\beta\|_2 = 1$  and recall that  $T_1 = \mathbb{P}(\beta^\top Z \leq 0 | Z_1 \geq 0)$ . Using the fact that both  $Z_1$  and  $Z_2$  are independent standard normal distributed random variables,

a simple geometric argument then yields that  $T_1 = \frac{\alpha}{\pi}$  with  $\alpha = \arccos\left(\frac{\beta_1}{\sqrt{\beta_1^2 + \beta_2^2}}\right) = \arccos(\beta_1)$ .

Noting that  $\beta_1 = \|\widehat{\Pi}_\parallel \theta^*\|_2 = \frac{\langle \theta^*, \theta \rangle}{\|\theta\|_2}$  then yields  $T_1 = \frac{1}{\pi} \arccos\left(\frac{\langle \theta^*, \theta \rangle}{\|\theta\|_2}\right)$ .

**Step 2: Proof for  $T_2$**  First, assume that  $\langle \theta^*, \theta \rangle \geq 0$ . We separate the event  $\mathcal{V} = \{Z_1 \leq \nu, b(Z_1, Z_2) \geq 0\}$  into two events  $\mathcal{V} = \mathcal{V}_1 \cup \mathcal{V}_2$

$$\mathcal{V}_1 = \{Z_1 \leq \nu, Z_2 \geq 0\} \quad \text{and} \quad \mathcal{V}_2 = \{Z_1 \leq \nu, b(Z_1, Z_2) \geq 0, Z_2 \leq 0\}.$$

The conditional probability of the first event is directly given

$$\mathbb{P}(\mathcal{V}_1 | Z_1 \geq 0) = \mathbb{P}(Z_2 \geq 0) \mathbb{P}(Z_1 \leq \nu | Z_1 \geq 0) = \frac{1}{2} \text{erf}\left(\frac{\nu}{\sqrt{2}}\right).$$

Hence it only remains to find an expression for  $\mathbb{P}(\mathcal{V}_2 | Z_1 \geq 0)$ . Letting  $\mu$  denote the standard normal distribution, we can write

$$\mathbb{P}(Z_1 \leq \nu, Z_2 \leq 0, b(Z_1, Z_2) \geq 0 | Z_1 \geq 0) = 2 \int_0^\nu \int_0^{\frac{\beta_1 x}{\beta_2}} d\mu(y) d\mu(x) = \int_0^\nu \frac{1}{2} \text{erf}\left(\frac{\beta_1 x}{\beta_2}\right) d\mu(x).$$

Together with Step 1, Equation (15) follows by noting that  $\beta_1^2 + \beta_2^2 = 1$ . Finally, the proof for the case where  $\langle \theta^*, \theta \rangle \leq 0$  follows exactly from the same argument and the proof is complete.  $\square$

### A.3 Distribution shift robustness and consistent adversarial robustness

In this section we introduce distribution shift robustness and show the relation to consistent  $\ell_p$ -adversarial robustness for certain types of distribution shifts.

When learned models are deployed in the wild, test and train distribution might not be the same. That is, the test loss might be evaluated on samples from a slightly different distribution than used to train the method. Shifts in the mean of the covariate distribution is a standard intervention studied in the invariant causal prediction literature [10, 11]. For mean shifts in the null space of the ground truth  $\theta^*$  we define an alternative evaluation metric that we refer to as the *distributionally robust risk* defined as follows:

$$\begin{aligned} \tilde{\mathbf{R}}_\epsilon(\theta) &:= \max_{\mathbb{Q} \in \mathcal{V}_q(\epsilon; \mathbb{P})} \mathbb{E}_{X \sim \mathbb{Q}} \ell_{\text{test}}(\langle \theta, X \rangle, \langle \theta^*, X \rangle), \text{ with} \\ \mathcal{V}_p(\epsilon; \mathbb{P}) &:= \{\mathbb{Q} \in \mathcal{P} : \|\mu_{\mathbb{P}} - \mu_{\mathbb{Q}}\|_p \leq \epsilon \text{ and } \langle \mu_{\mathbb{P}} - \mu_{\mathbb{Q}}, \theta^* \rangle = 0\}, \end{aligned}$$

where  $\mathcal{V}_p$  is the neighborhood of mean shifted probability distributions.

A duality between distribution shift robustness and adversarial robustness has been established in earlier work such as [48] for general convex, continuous losses  $\ell_{\text{test}}$ . For our setting, the following lemma holds.

**Lemma A.3.** *For any  $\epsilon \geq 0$  and  $\theta$ , we have  $\tilde{\mathbf{R}}_\epsilon(\theta) \leq \mathbf{R}_\epsilon(\theta)$ .*

*Proof.* The proof follows directly from the definition and consistency of the perturbations  $\mathcal{U}_p(\epsilon)$  and orthogonality of the mean shifts for the neighborhood  $\mathcal{V}_p$ . By defining the random variable  $W = X - \mu_{\mathbb{P}}$  for  $X \sim \mathbb{P}$  we have the distributional equivalence

$$X' = \mu_{\mathbb{Q}} + \delta + W \stackrel{d}{=} x + \delta$$

for  $X' \sim \mathbb{Q}$  and  $X \sim \mathbb{P}$  with  $\mu_{\mathbb{Q}} - \mu_{\mathbb{P}} = \delta$  and hence

$$\begin{aligned} \tilde{\mathbf{R}}_\epsilon(\theta) &= \max_{\mathbb{Q} \in \mathcal{V}_p(\epsilon)} \mathbb{E}_{X \sim \mathbb{Q}} \ell_{\text{test}}(\langle \theta, X \rangle, \langle \theta^*, X \rangle) = \max_{\|\delta\|_p \leq \epsilon, \delta \perp \theta^*} \mathbb{E}_{X \sim \mathbb{P}} \ell_{\text{test}}(\langle \theta, X + \delta \rangle, \langle \theta^*, X \rangle) \\ &\leq \mathbb{E}_{X \sim \mathbb{P}} \max_{\|\delta\|_p \leq \epsilon, \delta \perp \theta^*} \ell_{\text{test}}(\langle \theta, X + \delta \rangle, \langle \theta^*, X \rangle) = \mathbf{R}_\epsilon(\theta) \end{aligned}$$

where the first line follows from orthogonality of the mean-shift to  $\theta^*$ .  $\square$

## B Experimental details

In this section we provide additional details on our experiments. All our code including instructions and hyperparameters can be found here: [https://github.com/michaelaerni/interpolation\\_robustness](https://github.com/michaelaerni/interpolation_robustness).

### B.1 Neural networks on sanitized binary MNIST

Figure 1a shows that robust overfitting in the overparameterized regime also occurs for single hidden layer neural networks on an image dataset that we chose to be arguably devoid of noise. We consider binary classification of MNIST classes 1 vs 3 and further reduce variance by removing “difficult” samples. More precisely, we train networks of width  $p \in \{10^1, 10^2, 10^3\}$  on the full MNIST training data and discard all images that take at least one of the models more than 100 epochs of training to fit. While some recent work argues that such sanitation procedures can effectively mitigate robust overfitting [16], we still observe a significant gap between the best (early-stopped) and final test robust accuracies in Figure 1a.

We train all networks on a subset of  $n = 2 \times 10^3$  samples using plain mini-batch stochastic gradient descent with learning rate  $\nu_p = \sqrt{0.1/p}$  that we multiply by 0.1 after 300 epochs. This learning rate schedule minimizes the training loss efficiently; we did not perform tuning using test or validation data. For the robust test error, we approximate worst-case  $\ell_\infty$ -perturbations using 10-step SGD attacks on each test sample.

## B.2 Linear and logistic regression

If not mentioned otherwise, we use noiseless i.i.d. samples from our synthetic data model as described in Section 2.1 for our empirical simulations. We calculate all risks in closed-form without noise and, in the robust case, with consistent perturbations. However, we approximate the integral for the robust 0-1 risk in Theorem 4.1 using a numerical integral solver since we cannot obtain a solution analytically.

For linear regression, we always sample a training set of size  $n = 10^3$  and run zero-initialized gradient descent for  $2 \times 10^3$  iterations. The learning rate depends on the data dimension  $d$  as  $\nu_d = \sqrt{1/d}$ . Since we observed the training to be initially unstable for large overparameterization ratios  $d/n$ , we linearly increase the learning rate from zero during the first 250 gradient descent iterations. For evaluation, the linear regression robust population risk always uses consistent  $\ell_2$ -perturbations of radius  $\epsilon = 0.4$ . For the noisy case in Figure 1b we set  $\sigma^2 = 0.2$ .

We fit all logistic regression models except in Figure 4b by minimizing the (regularized) logistic loss from Equation (7) using *CVXPY* in combination with the *Mosek* convex programming solver. Whenever the max- $\ell_2$ -margin solution is feasible for  $\lambda \rightarrow 0$ , the problem in Equation (7) has many optimal solutions. In that case, we directly optimize the constrained problem from Equation (8) instead. For Figure 4b, we run zero-initialized gradient descent on the unregularized loss ( $\lambda = 0$ ) for  $5 \times 10^5$  iterations. We start with a small initial step size of 0.01 that we double every  $3 \times 10^4$  steps until iteration  $3 \times 10^5$ . Next, we perform all simulations in Figure 6 on  $n = 10^3$  samples from our data model with  $d = 8 \times 10^3$ . Both training and evaluation use consistent  $\ell_\infty$ -perturbations of radius  $\epsilon = 0.1$ . Lastly, for the noisy case in Figure 1c, we flip 2% of all training sample labels.

## B.3 Theoretical predictions

In order to obtain the asymptotic theoretical predictions for logistic regression in Figure 5b corresponding to the empirical simulations with  $n = 10^3$  and  $\epsilon = 0.05$ , we obtain the solution of the optimization problems in Theorem F.1,F.2 with  $\epsilon_0 = 0.05\sqrt{10^3\gamma}$  by solving the system of equations  $\nabla C = 0$  (with  $C$  the optimization objective from Theorem F.1,F.2) using *MATLAB*'s optimization toolbox where we approximate expectations via numerical integration. We note that the optimization problem is numerically challenging to solve, in particular for small values of  $\gamma$ .

## C Linear regression – additional insights

In this section we discuss how inconsistent adversarial training prevents interpolation for linear regression. As shown in [25] and using the same arguments as in Section A.1, the robust square loss under inconsistent  $\ell_2$ -perturbations can be reformulated as

$$\begin{aligned} \mathcal{L}_\epsilon(\theta) &= \frac{1}{n} \sum_{i=1}^n (|y_i - \langle x_i, \theta \rangle| + \epsilon \|\theta\|_2)^2 \\ &= \frac{1}{n} \sum_{i=1}^n (y_i - \langle x_i, \theta \rangle)^2 + \epsilon^2 \|\theta\|_2^2 + \frac{2\epsilon}{n} \|\theta\|_2 \sum_{i=1}^n |y_i - \langle x_i, \theta \rangle|. \end{aligned}$$

Thus, we can see that adversarial training with inconsistent perturbations prevents interpolation even when  $d > n$ , that is,  $\mathcal{L}_\epsilon(\theta) = 0$  is unattainable for any  $\epsilon > 0$ . Nevertheless, we note that optimizing the reformulated robust square loss is equivalent to  $\ell_2$ -regularized linear regression with  $\lambda = \epsilon^2$  and an additional term involving both the weight norm and absolute prediction residuals. We can observe this effect in Figure 4 of [25] where larger  $\epsilon$  yield similar effects to larger ridge penalties  $\lambda$ .

## D Logistic regression – additional insights

In this section we further discuss robust logistic regression studied in Section 4. Appendix D.1 presents further experiments to contrast consistent and inconsistent perturbations for adversarial training. Furthermore, for completeness, we investigate standard training (that is,  $\epsilon = 0$ ) in Section D.2 and note that it yields significantly worse standard and robust prediction performance.

## D.1 Inconsistent adversarial training

As observed in Section 4.4, label noise can prevent interpolation and hence improve the robust risk of an unregularized estimator with  $\lambda \rightarrow 0$ . We now show similar empirical effects of inconsistent training perturbations with large enough radius  $\epsilon$ .

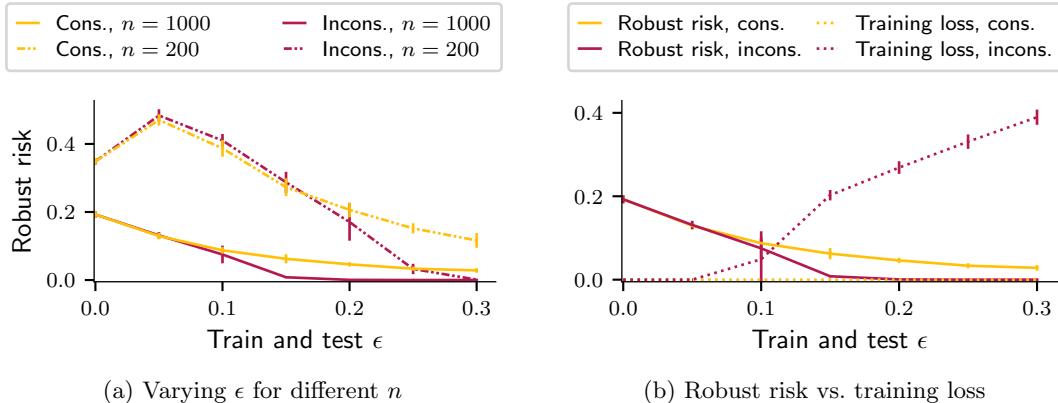


Figure 8: Comparison of logistic regression adversarial training with consistent vs. inconsistent  $\ell_\infty$ -perturbations. (a) Robust risks of the unregularized estimators ( $\lambda \rightarrow 0$ ) for  $n = 200, 1000$  as  $\epsilon$  increases. While for small  $\epsilon$ , consistent and inconsistent perturbations yield similar robust risks, inconsistent perturbations with large  $\epsilon$  outperform consistent perturbations in terms of robustness. We provide an explanation in (b) where we focus on  $n = 1000$ . In contrast to training with consistent perturbations, inconsistent perturbations may prevent the training loss from vanishing as  $\epsilon$  grows large enough. Hence, inconsistent training perturbations can induce spurious regularization effects. We average all experiments over five independent dataset draws from our data model with fixed  $d = 500$  and indicate one standard deviation via error bars.

Concretely, we perform unregularized ( $\lambda \rightarrow 0$ ) adversarial training using consistent vs. inconsistent  $\ell_\infty$ -perturbations for different  $\epsilon$  on fixed  $n = 200, 10^3$  and  $d = 500$ . Figure 8a displays the robust risks of the resulting estimators. For small  $\epsilon$ , all risks behave very similarly, further corroborating our observations in Figure 5a. However, as the perturbation radius  $\epsilon$  grows large, inconsistent perturbations for unregularized adversarial training yield estimators with better robust risk compared to consistent perturbations.

In order to understand this phenomenon, we focus on  $n = 10^3$  and depict the robust risk as well as the robust (unregularized) logistic training loss in Figure 8b. We observe that, for large  $\epsilon$ , inconsistent adversarial training fails to achieve a vanishing loss. Hence, large enough inconsistent perturbations induce noise which prevents interpolation. This observation is similar to the observation made in Section 4.4, where explicit label noise can have spurious regularization effects and in turn, lead to a lower robust risk.

## D.2 Standard vs. adversarial training

Throughout this paper, we focus on adversarial training for logistic regression. For completeness, we also provide simulation results for standard training ( $\epsilon = 0$ ) in Figure 9a. We again use a dataset of size  $n = 10^3$ . In contrast to adversarial training with  $\epsilon > 0$ , we do not observe overfitting for neither the standard nor robust risk. However, for  $d > n$ , the robust risk exhibits its maximum possible value and hence fails to provide any insights. We note that our observations are consistent with [46].

## D.3 Adversarial training with $\ell_2$ -perturbations

As mentioned in Section 4, we focus on  $\ell_\infty$ -perturbations in the context of logistic regression but for completeness also discuss  $\ell_2$ -perturbations. Following the same argument as in Lemma A.2, it is

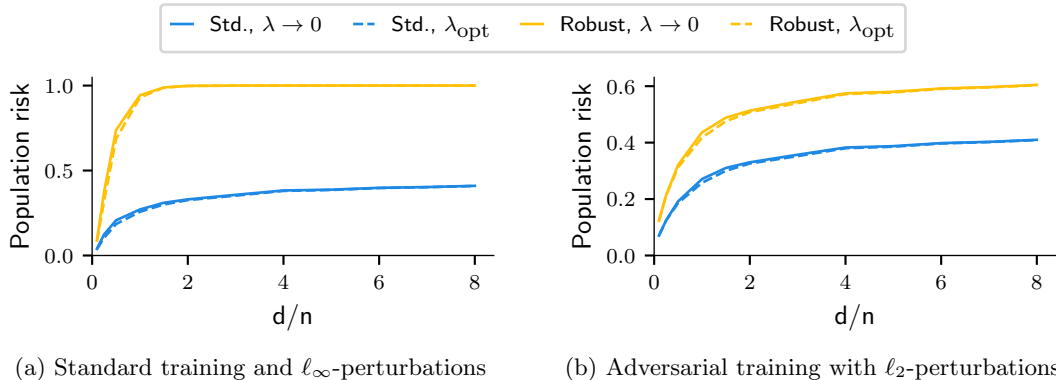


Figure 9: Additional logistic regression simulations using  $n = 10^3$  training samples from our data model for varying degrees of overparameterization  $d/n$ . (a) Standard training evaluated using consistent  $\ell_\infty$ -perturbations of radius  $\epsilon = 0.1$ . (b) Adversarial training using inconsistent  $\ell_2$ -perturbations of radius  $\epsilon = 0.5$  for training and the corresponding consistent perturbation set for evaluation. In both settings, the robust risks are large and not even an optimally weighted ridge penalty helps to reduce them.

trivial to see that  $\ell_2$ -perturbations punish the  $\ell_2$ -norm of the estimator. Intuitively, we therefore expect that adversarial training with  $\ell_2$ -perturbations results in an estimator  $\hat{\theta}_\lambda$  that is close to a rescaled version of the estimator obtained if training without adversarial perturbations. Since both the robust and standard risk are independent of the estimator scale, we hence do not expect any benefits from explicit  $\ell_2$ -regularization, i.e., no robust overfitting. Indeed, our simulation results in Figure 9b show almost no regularization benefits for neither the standard nor robust risk.

## E Proof of Theorem 3.1

In this section, we provide a proof of Theorem 3.1, which characterizes the asymptotic risk of the linear regression estimator  $\hat{\theta}_\lambda$  defined in Equation (3).

We first introduce some notation and give the standard closed form solution for the ridge regression estimate  $\hat{\theta}_\lambda$ . Denoting the input data matrix by  $X \in \mathbb{R}^{d \times n}$ , the observation vector  $y \in \mathbb{R}^n$  reads  $y = X^\top \theta^* + \xi$  where  $\xi \sim \mathcal{N}(0, I)$  is the noise vector. The noise vector contains i.i.d. zero-mean  $\sigma^2$ -variance Gaussian noise as entries. Defining the empirical covariance matrix as  $\hat{\Sigma} = \frac{1}{n} X^\top X$  yields the ridge estimate

$$\begin{aligned} \hat{\theta}_\lambda &= \frac{1}{n} (\lambda I_d + \hat{\Sigma})^{-1} X^\top y \\ &= (\lambda I_d + \hat{\Sigma})^{-1} \hat{\Sigma} \theta^* + \frac{1}{n} (\lambda I_d + \hat{\Sigma})^{-1} X^\top \xi. \end{aligned} \tag{19}$$

For  $\lambda \rightarrow 0$ , we obtain the min-norm interpolator

$$\hat{\theta}_0 = \lim_{\lambda \rightarrow 0} \hat{\theta}_\lambda = \hat{\Sigma}^\dagger X^\top y,$$

where  $\hat{\Sigma}^\dagger$  denotes the Moore-Penrose pseudo inverse.

We now compute the adversarial risk of this estimator. By Equation (12), the adversarial risk depends on the estimator only via the two terms  $\|\hat{\theta}_\lambda - \theta^*\|_2$  and  $\|\Pi_\perp \hat{\theta}_\lambda\|_2$ . To characterize the asymptotic risk, we hence separately derive asymptotic expressions for each of both terms. The following convergence results hold almost surely with respect to the draws of the train dataset, with input features  $X$  and observations  $y$ , as  $n, d \rightarrow \infty$ .



**Step 1: Characterizing  $\|\hat{\theta}_\lambda - \theta^*\|_2^2$ .** Here, we show that

$$\|\hat{\theta}_\lambda - \theta^*\|_2^2 \rightarrow \mathcal{R}_\lambda = \mathcal{B} + \mathcal{V}, \quad (20)$$

where  $\mathcal{B} = \lambda^2 m'(-\lambda)$  and  $\mathcal{V} = \sigma^2 \gamma(m(-\lambda) - \lambda m'(-\lambda))$  are the asymptotic bias and variance. Hastie et al. [23] considers a similar setup and Theorem 5 of [23] show that  $\mathbb{E}_\xi \|\hat{\theta}_\lambda - \theta^*\|_2^2 \rightarrow \mathcal{B} + \mathcal{V}$  and the expectation is taken over the observation noise  $\xi$  in the train dataset. In this paper, we define the population risks without the expectation over the noise. Hence, in a first step, the goal is to extend Theorem 5 [23] for the standard risk  $\mathbf{R}(\hat{\theta}_\lambda) = \|\hat{\theta}_\lambda - \theta^*\|_2^2$  such that (20) holds almost surely over the draws of the training data.

Using Equation (19) we can rewrite

$$\begin{aligned} \|\hat{\theta}_\lambda - \theta^*\|_2^2 &= \left\| \left( I_d - (\lambda I_d + \widehat{\Sigma})^{-1} \widehat{\Sigma} \right) \theta^* + \frac{1}{n} (\lambda I_d + \widehat{\Sigma})^{-1} \mathbf{X}^\top \xi \right\|_2^2 \\ &= \underbrace{\left\| \left( I_d - (\lambda I_d + \widehat{\Sigma})^{-1} \widehat{\Sigma} \right) \theta^* \right\|_2^2}_{T_1} + \underbrace{\left\langle \frac{\xi}{\sqrt{n}}, (\lambda I_d + \widehat{\Sigma})^{-2} \widehat{\Sigma} \frac{\xi}{\sqrt{n}} \right\rangle}_{T_2} \\ &\quad + \underbrace{\left\langle \frac{\mathbf{X}^\top}{\sqrt{n}} (\lambda I_d + \widehat{\Sigma})^{-1} \left( I_d - (\lambda I_d + \widehat{\Sigma})^{-1} \widehat{\Sigma} \right) \theta^*, \frac{\xi}{\sqrt{n}} \right\rangle}_{T_3}, \end{aligned}$$

where we used for the second equality that  $\left\langle \frac{\xi}{\sqrt{n}}, \frac{\mathbf{X}}{\sqrt{n}} (\lambda I_d + \widehat{\Sigma})^{-2} \frac{\mathbf{X}^\top}{\sqrt{n}} \frac{\xi}{\sqrt{n}} \right\rangle = \left\langle \frac{\xi}{\sqrt{n}}, (\lambda I_d + \widehat{\Sigma})^{-2} \widehat{\Sigma} \frac{\xi}{\sqrt{n}} \right\rangle$ .

The first term  $T_1 \rightarrow \mathcal{B}$  follows directly via Theorem 5 [23]. We next show that  $T_2 \rightarrow \mathcal{V}$  and  $T_3 \rightarrow 0$  almost surely, which establishes Equation 20.

**Proof that  $T_2 \rightarrow \mathcal{V}$ :** While Theorem 5 [23] also shows that  $\mathbb{E}_\xi \text{tr} \left( \frac{1}{n} \xi \xi^\top \widehat{\Sigma} (\lambda I_d + \widehat{\Sigma})^{-2} \right) \rightarrow \mathcal{V}$ , we require the convergence almost surely over a single draw of  $\xi$ . In fact, this directly follows from the same argument as used for the proof of Theorem 5 [23] and the fact that  $\|\frac{\xi}{\sqrt{n}}\|_2^2 \rightarrow \sigma^2$ . Hence  $\left\langle \frac{\xi}{\sqrt{n}}, (\lambda I_d + \widehat{\Sigma})^{-2} \widehat{\Sigma} \frac{\xi}{\sqrt{n}} \right\rangle \rightarrow \mathcal{V}$  almost surely over the draws of  $\xi$ .

**Proof that  $T_3 \rightarrow 0$ :** This follows straight forwardly from sub-Gaussian concentration inequalities and from the fact that

$$\left\| \frac{\mathbf{X}}{\sqrt{n}} (\lambda I_d + \widehat{\Sigma})^{-1} \left( I_d - (\lambda I_d + \widehat{\Sigma})^{-1} \widehat{\Sigma} \right) \theta^* \right\|_2 = O(1),$$

which is a direct consequence of the Bai-Yin theorem [4], stating that for sufficiently large  $n$ , the non zero eigenvalues of  $\widehat{\Sigma}$  can be almost surely bounded by  $(1 + \sqrt{\gamma})^2 \geq \lambda_{\max}(\widehat{\Sigma}) \geq \lambda_{\min}(\widehat{\Sigma}) \geq (1 - \sqrt{\gamma})^2$ . Hence we can conclude the first part of the proof.

**Step 2: Characterizing  $\|\Pi_\perp \hat{\theta}_\lambda\|_2$ .** Here, we show that

$$\|\Pi_\perp \hat{\theta}_\lambda\|_2^2 \rightarrow \mathcal{R}_\lambda - \lambda^2 (m(-\lambda))^2 =: \mathcal{P}_\lambda. \quad (21)$$

We assume without loss of generality that  $\|\theta^*\|_2 = 1$  and hence  $\Pi_\perp = I_d - \theta^* (\theta^*)^\top$ . It follows that

$$\begin{aligned} \|\Pi_\perp \hat{\theta}_\lambda\|_2^2 &= \|\hat{\theta}_\lambda\|_2^2 - \left( \langle \hat{\theta}_\lambda, \theta^* \rangle \right)^2 \\ &= \|\theta^* - \hat{\theta}_\lambda - \theta^*\|_2^2 - \left( 1 - \langle \theta^* - \hat{\theta}_\lambda, \theta^* \rangle \right)^2 \\ &= \|\theta^* - \hat{\theta}_\lambda\|_2^2 - 2 \langle \theta^* - \hat{\theta}_\lambda, \theta^* \rangle + 1 - \left( 1 - \langle \theta^* - \hat{\theta}_\lambda, \theta^* \rangle \right)^2 \\ &= \|\theta^* - \hat{\theta}_\lambda\|_2^2 - \left( \langle \theta^* - \hat{\theta}_\lambda, \theta^* \rangle \right)^2. \end{aligned}$$

The convergence of the first term is already known from step 1. Hence, it is only left to find an asymptotic expression for  $\langle \theta^* - \hat{\theta}_\lambda, \theta^* \rangle$ . Inserting the closed form expression from Equation (19), we obtain:

$$\langle \theta^* - \hat{\theta}_\lambda, \theta^* \rangle = \langle I_d - (\lambda I_d + \widehat{\Sigma})^{-1} \widehat{\Sigma} \rangle \theta^*, \theta^* \rangle - \langle (\lambda I_d + \widehat{\Sigma})^{-1} \frac{X^\top \xi}{n}, \theta^* \rangle. \quad (22)$$

Note that  $\langle (\lambda I_d + \widehat{\Sigma})^{-1} \frac{X^\top \xi}{n}, \theta^* \rangle$  vanishes almost surely over the draws of  $\xi$  using the same reasoning as in the first step. Hence, we only need to find an expression for the first term on the RHS of Equation (22). Note that we can use Woodbury's matrix identity to write:

$$\langle I_d - (\lambda I_d + \widehat{\Sigma})^{-1} \widehat{\Sigma} \rangle \theta^*, \theta^* \rangle = \lambda \langle (\lambda I_d + \widehat{\Sigma})^{-1} \theta^*, \theta^* \rangle.$$

However, the expression on the RHS appears exactly in the proof of Theorem 1 [23] (Equation 116), which shows that  $\lambda \langle (\lambda I_d + \widehat{\Sigma})^{-1} \theta^*, \theta^* \rangle \rightarrow \lambda m(-\lambda)$  with  $m(z)$  as in Theorem 3.1. Hence the proof of almost sure convergence (21) of  $\|\Pi_\perp \hat{\theta}_\lambda\|_2$  is complete.

Substituting Equations (20) and (21) into robust risk (12) expression yields:

$$\mathbf{R}_\epsilon(\hat{\theta}_\lambda) \xrightarrow{\text{a.s.}} \mathcal{R}_\lambda + \epsilon^2 \mathcal{P}_\lambda + \sqrt{\frac{8\epsilon^2}{\pi} \mathcal{P}_\lambda \mathcal{R}_\lambda} = \mathcal{R}_{\epsilon, \lambda}.$$

Finally, we note that  $\lim_{\lambda \rightarrow 0} \mathcal{R}_{\epsilon, \lambda}$  exists and is finite for any  $\gamma \neq 1$  since:  $\lim_{\lambda \rightarrow 0} m(-z) = \frac{1}{1-\gamma}$  for  $\gamma < 1$  and  $\lim_{\lambda \rightarrow 0} m(-z) = \frac{1}{\gamma(\gamma-1)}$  for  $\gamma > 1$ ,  $\lim_{z \rightarrow 0} z m'(-z) = 0$ ,  $\lim_{z \rightarrow 0} z^2 m'(-z) = 0$  for  $\gamma < 1$  and  $\lim_{z \rightarrow 0} z^2 m'(-z) = 1 - \frac{1}{\gamma}$  for  $\gamma > 1$  (see also Corollary 5 in [23]). Hence, we can conclude from the continuity of the risk that  $\mathbf{R}_\epsilon(\hat{\theta}_0) \xrightarrow{\text{a.s.}} \lim_{\lambda \rightarrow 0} \mathcal{R}_{\epsilon, \lambda}$  and therefore, the proof is complete.

## F Details on Theorem 4.1

In this section we give a formal statement for Theorem 4.1. The results are based on the Convex Gaussian Minimax Theorem (CGMT) [20, 51]. We first prove the case when training with consistent perturbations (10) and noiseless observations. Then, we show how the theorems extend to the case when training with inconsistent perturbations (9) and training label noise.

The results presented in this section have similarities with the ones in [24]. However, we study a discriminative data model with features drawn from a single Gaussian and a 1-sparse ground truth. In contrast, the authors of [24] study a generative data model with features drawn from two Gaussians. Furthermore, several papers study logistic regression for isotropic Gaussian features in high dimensions [46, 50], but focus their analysis on the standard risk and do not consider adversarial robustness.

An immediate consequence of the proof of Lemma A.2 is that the adversarial loss from Equation (7) with respect to consistent  $\ell_\infty$ -attacks (10) for the 1-sparse ground truth has the closed-form equivalent

$$\mathcal{L}_{\epsilon, \lambda}(\theta) = \frac{1}{n} \sum_{i=1}^n \ell_{\text{train}}(y_i \langle \theta, x_i \rangle - \epsilon \|\Pi_\perp \hat{\theta}\|_1) + \lambda \|\theta\|_2^2, \quad (23)$$

where  $\Pi_\perp$  is the projection matrix to the orthogonal subspace of  $\theta^*$ .

Let  $\mathcal{M}_f(x, t) = \min_y \frac{1}{2t} (x - y)^2 + f(y)$  be the Moreau envelope and let  $Z_\parallel, Z_\perp$  be two independent standard normal random variables. We can now state Theorem F.1 that describes the asymptotic risk of  $\hat{\theta}_\lambda(\epsilon)$ , for  $\lambda > 0$  and for the asymptotic regime where  $d, n \rightarrow \infty$ . The proof of the theorem can be found in Appendix F.1.

**Theorem F.1.** *Assume that we have i.i.d. random features  $x_i$  drawn from an isotropic Gaussian, noiseless observations  $y_i = \text{sgn}(\langle x_i, \theta^* \rangle)$ , and ground truth  $\theta^* = (1, 0, \dots, 0)^\top$ . Further, assume that  $\lambda > 0$  and  $\epsilon = \epsilon_0 / \sqrt{d}$ , where  $\epsilon_0$  is a numerical constant. Let  $(\nu_\perp^*, \nu_\parallel^*, r^*, \delta^*, \mu^*, \tau^*)$  be the unique*

solution of

$$\begin{aligned} & \min_{\substack{\nu_{\perp} \geq 0, \tau \geq 0, \\ \nu_{\parallel}, \delta \geq 0}} \max_{\substack{r \geq 0, \\ \mu \geq 0}} \mathbb{E}_{Z_{\parallel}, Z_{\perp}} \left[ \mathcal{M}_{\ell}(|Z_{\parallel}| \nu_{\parallel} + Z_{\perp} \nu_{\perp} - \epsilon_0 \delta, \frac{\tau}{r}) \right] - \delta \mu + \frac{r\tau}{2} + \lambda(\nu_{\perp}^2 + \nu_{\parallel}^2) \\ & - \nu_{\perp} \sqrt{\left[ (\mu^2 + \gamma r^2) - (\mu^2 + \gamma r^2) \operatorname{erf}(\mu/(\sqrt{\gamma} r \sqrt{2})) - \sqrt{\frac{2}{\pi}} \sqrt{\gamma} r \mu \exp(-\mu^2/(\gamma r^2 2)) \right]}. \end{aligned} \quad (24)$$

Then, for  $\lambda > 0$ , the estimator  $\hat{\theta}_{\lambda}(\epsilon)$  from Equation (7) with the logistic loss and consistent  $\ell_{\infty}$ -perturbations satisfies asymptotically as  $d, n \rightarrow \infty$  and  $d/n \rightarrow \gamma$  that

$$\frac{1}{\sqrt{d}} \|\Pi_{\perp} \hat{\theta}_{\lambda}(\epsilon)\|_1 \rightarrow \delta^* \quad \text{and} \quad \langle \hat{\theta}_0(\epsilon), \theta^* \rangle \rightarrow \nu_{\parallel}^* \quad \text{and} \quad \|\hat{\theta}_{\lambda}(\epsilon)\|_2^2 \rightarrow \nu_{\parallel}^{*2} + \nu_{\perp}^{*2}. \quad (25)$$

The convergences hold in probability.

For  $\lambda > 0$ , the loss in Equation (23) has a unique minimizer. In contrast, for  $\lambda = 0$ , the minimizer of Equation (23) is not unique. In the latter case, we study the robust max- $\ell_2$ -margin solution from Equation (8), which corresponds to the limit when  $\lambda \rightarrow 0$  (see Section 4.1). Theorem F.2 characterizes the asymptotic behavior of the corresponding solution, with proof in Appendix F.2.

**Theorem F.2.** *Assume that we have i.i.d. random features  $x_i$  drawn from an isotropic Gaussian, noiseless observations  $y_i = \operatorname{sgn}(\langle x_i, \theta^* \rangle)$ , and  $\theta^* = (1, 0, \dots, 0)^{\top}$ . Further, assume that  $\lambda = 0$  and  $\epsilon = \epsilon_0/\sqrt{d}$ , where  $\epsilon_0$  is a numerical constant. Let  $(\nu_{\perp}^*, \nu_{\parallel}^*, r^*, \delta^*, \zeta^*, \kappa^*, \tau^*)$  be the unique solution of*

$$\begin{aligned} & \max_{\substack{r \geq 0, \nu_{\perp} \geq 0, \\ \zeta \geq 0}} \min_{\substack{\nu_{\parallel} \geq 0, \\ \delta \geq 0}} \max_{\kappa \geq 0} \min_{\tau \geq 0} \nu_{\parallel}^2 - \kappa \nu_{\perp} - \delta \zeta - \frac{\gamma r^2}{4(1 + \frac{\kappa}{2\tau})} \\ & + r \sqrt{\mathbb{E}_{Z_{\parallel}, Z_{\perp}} \left[ \max(0, 1 + \epsilon_0 \delta - |Z_{\parallel}| \nu_{\parallel} + Z_{\perp} \nu_{\perp})^2 \right]} \\ & + \frac{1}{2(1 + \frac{\kappa}{2\tau})} \left( \frac{\gamma r^2 + \zeta^2}{2} \operatorname{erf} \left( \frac{\zeta}{\sqrt{2} \sqrt{\gamma} r} \right) - \frac{\zeta^2}{2} + \frac{\sqrt{\gamma} r \zeta}{\sqrt{2\pi}} \exp \left( -\frac{\zeta^2}{2\gamma r^2} \right) \right) + \frac{\kappa \tau}{2}. \end{aligned} \quad (26)$$

Then, the estimator  $\hat{\theta}_0(\epsilon)$  from Equation (8) with the logistic loss and consistent  $\ell_{\infty}$ -perturbations satisfies asymptotically as  $d, n \rightarrow \infty$  and  $d/n \rightarrow \gamma$  that

$$\frac{1}{\sqrt{d}} \|\Pi_{\perp} \hat{\theta}_0(\epsilon)\|_1 \rightarrow \delta^* \quad \text{and} \quad \langle \hat{\theta}_0(\epsilon), \theta^* \rangle \rightarrow \nu_{\parallel}^* \quad \text{and} \quad \|\hat{\theta}_0(\epsilon)\|_2^2 \rightarrow \nu_{\parallel}^{*2} + \nu_{\perp}^{*2}. \quad (27)$$

The convergences hold in probability.

**Remark F.3.** *Theorem 4.1 follows from Theorems F.1 and F.2 when inserting the expression from Equations (25),(27) into the expression of the risk in Lemma A.2.*

**Inconsistent adversarial attacks** We now show that Theorems F.1,F.2 also hold when training with inconsistent attacks (9).

For inconsistent adversarial attacks, we simply need to change  $\epsilon \|\Pi_{\perp} \theta\|_1$  to  $\epsilon \|\theta\|_1 = \epsilon \|\Pi_{\perp} \theta\|_1 + \epsilon \|\Pi_{\parallel} \theta\|_1$  in the optimization objective in Equations (28),(38). To show that these modifications do not change the asymptotic solution as  $d, n \rightarrow \infty$ , note that  $\epsilon \|\Pi_{\parallel} \theta\|_1 = \frac{\epsilon_0}{\sqrt{n}} \|\Pi_{\parallel} \theta\|_1 \rightarrow 0$  which follows from the fact that  $\|\Pi_{\parallel} \theta\|_1$  remains bounded as  $d, n \rightarrow \infty$ .

**Label noise** While our results assume noiseless observations  $y_i = \operatorname{sgn}(\langle x_i, \theta^* \rangle)$ , Theorem F.1,F.2 can be extended to the case where additional label noise is added to the observations. That is, we observe  $y_i = \operatorname{sgn}(\langle x_i, \theta^* \rangle) \xi_i$  with  $\xi_i$  i.i.d.,  $\mathbb{P}(\xi_i = 1) = 1 - \sigma$  and  $\mathbb{P}(\xi_i = -1) = \sigma$ , where  $\sigma$  is the strength of the label noise.

Note that, as discussed in Section D.1, the robust max-margin solution (8) might not exist for noisy observations. In that case, the robust logistic regression estimate (7) has a unique solution for  $\lambda = 0$ . In fact, following the same argument as in [24], asymptotically, we can find a threshold  $\gamma^*$  such that for any  $\gamma < \gamma^*$ , the robust max- $\ell_2$ -margin solution does not exist, and for any  $\gamma \geq \gamma^*$ , the robust max- $\ell_2$ -margin solution exists. The threshold can be found using the CGMT when following the same argument as in Theorem 6.1 of [24].

Finally, we remark that, when  $\lambda > 0$  or  $\lambda = 0$  and  $\gamma < \gamma^*$ , we can extend Theorem F.1 by replacing  $|Z_{\parallel}|$  with  $\xi|Z_{\parallel}|$ , where  $\xi$  is drawn from the same distribution as  $\xi_i$  defined above. Similarly, for  $\lambda = 0$  and  $\gamma \geq \gamma^*$ , we can extend Theorem F.2 by replacing  $|Z_{\parallel}|$  with  $\xi|Z_{\parallel}|$ .

**Outline of the proof** The proof of Theorems F.1, F.2 heavily relies on the proofs of Theorem 6.3 and 6.4 in [24]. In particular, our proof essentially follows the same structure by first reducing the problem via an application of the Lagrange multiplier to an expression that suits the CGMT framework. This allows us to instead study the auxiliary optimization problem as described in Equation (31), which we then simplify to a scalar optimization problem using standard concentration inequalities of Gaussian random variables.

The major difference to Theorems 6.3 and 6.4 in [24] is that we study a discriminative data model with a sparse ground truth, whereas Theorem 6.3 and 6.4 in [24] assume a generative data model and, in particular, do not allow sparse ground truth vectors  $\theta^*$ . This is due to the different attack sizes as we choose  $\epsilon = \epsilon_0/\sqrt{d}$  while Theorems 6.3 and 6.4 in [24] assume a constant attack size  $\epsilon = \epsilon_0$ .

## F.1 Proof of Theorem F.1

Denote with  $X \in \mathbb{R}^{n \times d}$  the input data matrix and with  $y \in \mathbb{R}^n$  the vector containing the observations. Recall that the estimator  $\hat{\theta}$  is given by

$$\begin{aligned} \hat{\theta} &= \arg \min_{\theta} \frac{1}{n} \sum_{i=1}^n \ell(y_i \langle x_i, \theta \rangle - \epsilon \|\Pi_{\perp} \theta\|_1) + \lambda \|\theta\|_2^2 \\ &= \arg \min_{\theta, v} \frac{1}{n} \sum_{i=1}^n \ell(v_i - \epsilon \|\Pi_{\perp} \theta\|_1) + \lambda \|\theta\|_2^2 \quad \text{such that } v = D_y X \theta, \end{aligned} \quad (28)$$

where  $\ell(x) = \log(1 + \exp(-x))$  is the logistic loss,  $X \in \mathbb{R}^{n \times d}$  is the data matrix and  $D_y$  the diagonal matrix with entries  $(D_y)_{i,i} = y_i$ . We can then introduce the Lagrange multipliers  $u \in \mathbb{R}^n$  to obtain

$$\min_{\theta, v} \max_u \frac{1}{n} \sum_{i=1}^n \ell(v_i - \epsilon \|\Pi_{\perp} \theta\|_1) + \frac{1}{n} u^{\top} D_y X \theta - \frac{1}{n} u^{\top} v + \lambda \|\theta\|_2^2.$$

Furthermore, we can separate  $X = X\Pi_{\perp} + X\Pi_{\parallel}$ , which yields

$$\min_{\theta, v} \max_u \frac{1}{n} \sum_{i=1}^n \ell(v_i - \epsilon \|\Pi_{\perp} \theta\|_1) + \frac{1}{n} u^{\top} D_y X \Pi_{\parallel} \theta + \frac{1}{n} u^{\top} D_y X \Pi_{\perp} \theta - \frac{1}{n} u^{\top} v + \lambda \|\theta\|_2^2. \quad (29)$$

**Convex Gaussian Minimax Theorem** We can now make use of the CGMT, which states that

$$\min_{\theta \in U_{\theta}} \max_{u \in U_u} u^{\top} X \theta + \psi(u, \theta), \quad (30)$$

with  $\psi$  convex in  $\theta$  and concave in  $u$ , has asymptotically, when  $d, n \rightarrow \infty$ ,  $d/n \rightarrow \gamma$ , pointwise the same solution as

$$\min_{\theta \in U_{\theta}} \max_{u \in U_u} \|u\|_2 g^{\top} \theta + u^{\top} h \|\theta\|_2 + \psi(u, \theta), \quad (31)$$

where  $g \in \mathbb{R}^d$  and  $h \in \mathbb{R}^n$  are random vectors with i.i.d. standard normal entries, and  $U_{\theta}$  and  $U_u$  are compact sets. As is common in the literature, we call Equation (30) the primal optimization problem and Equation (31) the auxiliary optimization problem. Several works have already used

the CGMT to study high dimensional asymptotic logistic regression [46], also when training with adversarial attacks [24]. We omit the precise statement and refer the reader to [51]. However, we note that we can apply the CGMT due to the following observations:

1. The objective (29) is concave in  $u$  and convex in  $v, \theta$ .
2. We can restrict  $u, v, \theta$  to compact sets without changing the solution. For  $\theta$ , we note that this is a consequence of  $\lambda > 0$ , and for  $u, v$ , we note that the stationary condition requires  $u_i = \ell'(v_i - \epsilon \|\Pi_{\perp} \theta\|_1)$ .
3.  $X\Pi_{\perp}$  is independent of the observations  $y$  and of  $X\Pi_{\parallel}$ .

Therefore, as a consequence of the CGMT, we can show that the solution of the primal optimization problem (29) asymptotically concentrates around the same value as the solution of the following auxiliary optimization problem:

$$\begin{aligned} \min_{\theta, v} \max_u \frac{1}{n} \sum_{i=1}^n \ell(v_i - \epsilon \|\Pi_{\perp} \theta\|_1) + \frac{1}{n} u^{\top} D_y X \Pi_{\parallel} \theta + \frac{1}{n} \|u^{\top} D_y\|_2 g^{\top} \Pi_{\perp} \theta \\ + \frac{1}{n} u^{\top} D_y h \|\Pi_{\perp} \theta\|_2 - \frac{1}{n} u^{\top} v + \lambda \|\theta\|_2^2, \end{aligned}$$

where  $g \in \mathbb{R}^d$  and  $h \in \mathbb{R}^n$  are vectors with i.i.d. standard normal entries.

**Scalarization of the optimization problem** We now aim to simplify the optimization problem. In a first step, we maximize over  $u$ . For this, define  $r = \|u\|_2 / \sqrt{n}$ , which allows us to equivalently write

$$\min_{\theta, v} \max_{r \geq 0} \frac{1}{n} \sum_{i=1}^n \ell(v_i - \epsilon \|\Pi_{\perp} \theta\|_1) + \frac{r}{\sqrt{n}} \|D_y X \Pi_{\parallel} \theta + D_y h \|\Pi_{\perp} \theta\|_2 - v\|_2 + \frac{1}{\sqrt{n}} r g^{\top} \Pi_{\perp} \theta + \lambda \|\theta\|_2^2,$$

where we have used the fact that  $\|u^{\top} D_y\|_2 = \|u\|_2$ . In order to proceed, we want to separate  $\Pi_{\perp} \theta$  from the loss  $\ell(v, \Pi_{\perp} \theta) := \frac{1}{n} \sum_{i=1}^n \ell(v_i - \epsilon \|\Pi_{\perp} \theta\|_1)$ . Denoting the conjugate of  $\ell$  by  $\tilde{\ell}$ , we can write  $\ell(v, \Pi_{\perp} \theta)$  in terms of its conjugate with respect to  $\Pi_{\perp} \theta$ :

$$\begin{aligned} \ell(v, \Pi_{\perp} \theta) &= \sup_w \frac{1}{\sqrt{d}} w^{\top} \Pi_{\perp} \theta - \tilde{\ell}(v, w) \\ &= \sup_w \frac{1}{\sqrt{d}} w^{\top} \Pi_{\perp} \theta - \sup_{\delta \geq 0} \left( \frac{\sqrt{d}}{\sqrt{d}} \delta \|w\|_{\infty} - \frac{1}{n} \sum_{i=1}^n \ell(v_i - \sqrt{d} \epsilon \delta) \right) \\ &= \sup_w \inf_{\delta \geq 0} \frac{1}{\sqrt{d}} w^{\top} \Pi_{\perp} \theta - \delta \|w\|_{\infty} + \frac{1}{n} \sum_{i=1}^n \ell(v_i - \epsilon_0 \delta), \end{aligned}$$

where, for the second identity, we use the derivation for the conjugate of  $\ell$  from Lemma A.2 in the paper [24]. Hence, we obtain:

$$\max_{r \geq 0} \min_{\theta, v} \max_w \min_{\delta \geq 0} \frac{1}{n} \sum_{i=1}^n \ell(v_i - \epsilon_0 \delta) + \frac{r}{\sqrt{n}} \|D_y X \Pi_{\parallel} \theta + D_y h \|\Pi_{\perp} \theta\|_2 - v\|_2 + \lambda \|\theta\|_2^2 \quad (32)$$

$$+ \frac{1}{\sqrt{d}} w^{\top} \Pi_{\perp} \theta - \delta \|w\|_{\infty} + \frac{1}{\sqrt{n}} r g^{\top} \Pi_{\perp} \theta. \quad (33)$$

In particular, note that the problem is concave in  $r, w$  and convex in  $\theta, v, \delta$ . Thus, we can interchange the order of maximization and minimization:

$$\begin{aligned} \max_{r \geq 0} \min_v \min_{\delta \geq 0} \max_w \min_{\theta} \frac{1}{n} \sum_{i=1}^n \ell(v_i - \epsilon_0 \delta) + \frac{r}{\sqrt{n}} \|D_y X \Pi_{\parallel} \theta + D_y h \|\Pi_{\perp} \theta\|_2 - v\|_2 + \lambda \|\theta\|_2^2 \quad (34) \\ + \frac{1}{\sqrt{d}} w^{\top} \Pi_{\perp} \theta - \delta \|w\|_{\infty} + \frac{1}{\sqrt{n}} r g^{\top} \Pi_{\perp} \theta. \end{aligned}$$

Next, we simplify the optimization over  $\theta$ . Write  $\Pi_{\parallel}\theta = \Pi_{\parallel}1\nu_{\parallel}$  with  $\nu_{\parallel} \in \mathbb{R}$  (here we use the fact that  $\theta^* = (1, 0, \dots, 0)$ ) and let  $\nu_{\perp} = \|\Pi_{\perp}\theta\|_2$ . We can simplify:

$$\begin{aligned} \max_{r \geq 0} \min_{\substack{\nu_{\perp} \geq 0, \\ \delta \geq 0, \\ \nu_{\parallel}, v}} \max_w & \frac{1}{n} \sum_{i=1}^n \ell(v_i - \epsilon_0 \delta) + \frac{r}{\sqrt{n}} \|D_y X \Pi_{\parallel} 1\nu_{\parallel} + D_y h \nu_{\perp} - v\|_2 + \lambda(\nu_{\parallel}^2 + \nu_{\perp}^2) \\ & - \frac{1}{\sqrt{d}} \nu_{\perp} \|\Pi_{\perp}(w - \sqrt{\gamma} r g)\|_2 - \delta \|w\|_{\infty} \end{aligned} \quad (35)$$

In order to obtain a low dimensional scalar optimization problem, we still need to scalarize the optimization over  $w$  and  $v$ . For this, we replace the term  $\|D_y X \Pi_{\parallel} 1\nu_{\parallel} + D_y h \nu_{\perp} - v\|_2$  with its square, which is achieved by using the following identity  $\min_{\tau \geq 0} \frac{x^2}{2\tau} + \frac{\tau}{2} = x$ . Hence,

$$\begin{aligned} \max_{r \geq 0} \min_{\substack{\nu_{\perp} \geq 0, \tau \geq 0, \\ \delta \geq 0, \\ \nu_{\parallel}, v}} & \frac{1}{n} \sum_{i=1}^n \ell(v_i - \epsilon_0 \delta) + \frac{r}{2\tau n} \|D_y X \Pi_{\parallel} 1\nu_{\parallel} + D_y h \nu_{\perp} - v\|_2^2 + \frac{\tau r}{2} + \lambda(\nu_{\parallel}^2 + \nu_{\perp}^2) \\ & + \max_w \left[ -\frac{1}{\sqrt{d}} \nu_{\perp} \|\Pi_{\perp}(w - \sqrt{\gamma} r g)\|_2 - \delta \|w\|_{\infty} \right]. \end{aligned}$$

We can now separately solve the following two inner optimization problems:

$$\max_w -\nu_{\perp} \frac{1}{\sqrt{d}} \|\Pi_{\perp}(w - \sqrt{\gamma} r g)\|_2 - \delta \|w\|_{\infty} \quad (36)$$

$$\min_v \frac{r}{2\tau n} \|D_y X \Pi_{\parallel} 1\nu_{\parallel} + D_y h \nu_{\perp} - v\|_2^2 + \sum_{i=1}^n \ell(v_i - \epsilon_0 \delta) \quad (37)$$

**Equation (36)** Let  $\text{ST}_t(x) = \begin{cases} 0 & |x| \leq t \\ \text{sgn}(x)(|x| - t) & \text{else} \end{cases}$  be the soft threshold function. We have

$$\begin{aligned} & \max_w -\nu_{\perp} \frac{1}{\sqrt{d}} \|\Pi_{\perp}(w - \sqrt{\gamma} r g)\|_2 - \delta \|w\|_{\infty} \\ & = -\min_w \nu_{\perp} \frac{1}{\sqrt{d}} \|\Pi_{\perp}(w - \sqrt{\gamma} r g)\|_2 + \delta \|w\|_{\infty} \\ & \stackrel{\mu = \|w\|_{\infty}}{=} -\min_{\mu \geq 0} \nu_{\perp} \sqrt{\frac{1}{d} \sum_{i=2}^d (\text{ST}_{\mu}(\sqrt{\gamma} r g_i))^2} + \delta \mu \\ & \stackrel{\text{LLN as } d \rightarrow \infty}{\rightarrow} -\min_{\mu \geq 0} \nu_{\perp} \sqrt{\mathbb{E}_Z (\text{ST}_{\mu}(\sqrt{\gamma} r Z))^2} + \delta \mu, \end{aligned}$$

where we used in the third line that the ground truth  $\theta^*$  is 1-sparse and in the last line that the expectation exists for  $Z \sim \mathcal{N}(0, 1)$ . Finally, we can further simplify

$$\begin{aligned} \mathbb{E}_Z (\text{ST}_{\mu}(\sqrt{\gamma} r Z))^2 & = \gamma r^2 \mathbb{E}_Z (\text{ST}_{\mu/(\sqrt{\gamma} r)}(Z))^2 \\ & = \gamma r^2 \mathbb{E}_Z (Z - \mu/(\sqrt{\gamma} r))^2 - \mathbb{E}_Z \mathbb{1}_{|Z| \leq \mu/(\sqrt{\gamma} r)} (Z - \mu/(\sqrt{\gamma} r))^2 \\ & = (\mu^2 + \gamma r^2) \left(1 - \text{erf}(\mu/(\sqrt{2\gamma} r))\right) - \sqrt{\gamma} r \mu \sqrt{\frac{2}{\pi}} \exp(-\mu/(2\gamma r^2)). \end{aligned}$$

Hence, we can conclude the first term.

**Equation (37)** For the second term we also aim to apply the law of large numbers. We have

$$\begin{aligned}
& \min_v \frac{r}{2\tau n} \|D_y \text{XII}_{\parallel} 1\nu_{\parallel} + D_y h\nu_{\perp} - v\|_2^2 + \frac{1}{n} \sum_{i=1}^n \ell(v_i - \epsilon_0 \delta) \\
& \stackrel{\tilde{v}=v-\epsilon_0\delta}{=} \min_{\tilde{v}} \frac{r}{2\tau n} \|D_y \text{XII}_{\parallel} 1\nu_{\parallel} + D_y h\nu_{\perp} - \tilde{v} - \epsilon_0 \delta\|_2^2 + \frac{1}{n} \sum_{i=1}^n \ell(\tilde{v}_i) \\
& = \min_{\tilde{v}} \frac{1}{n} \sum_{i=1}^n \frac{r}{2\tau n} \left( (D_y \text{XII}_{\parallel} 1\nu_{\parallel})_i + (D_y h\nu_{\perp})_i - \tilde{v}_i - \epsilon_0 \delta \right)^2 + \ell(\tilde{v}_i) \\
& \stackrel{\text{LLN}}{\rightarrow} \mathbb{E}_{Z_{\parallel}, Z_{\perp}} \left[ \mathcal{M}_{\ell}(|Z_{\parallel}| \nu_{\parallel} + Z_{\perp} \nu_{\perp} - \epsilon_0 \delta, \frac{\tau}{r}) \right],
\end{aligned}$$

where in the last line we used that  $(D_y \text{XII}_{\parallel} 1)_i = y_i x_i^{\top} \theta^* = \text{sgn}(x_i^{\top} \theta^*) x_i^{\top} \theta^*$  has the same distribution as  $|Z_{\parallel}|$  with  $Z_{\parallel} \sim \mathcal{N}(0, 1)$ . Further, to apply the law of large numbers, we need to show that the Moreau envelope exists. Similarly to Theorem 1 [46], this follows immediately when noting that  $\mathcal{M}_{\ell}(x, \mu) \leq \ell(x) = \log(1 + \exp(-x)) \leq \log(2) + |x|$ . Finally, we obtain the desired optimization problem in Equation (24) when combining these results.

**Convergence** One can check that the optimization problems defined in Equations (24),(28) are convex in the variables that we minimize over, and concave in the variables that we maximize over. Indeed, Equation (28) is immediate and Equation (24) follows straightforwardly from the fact that the problem in Equation (32) is convex and concave as desired. Therefore, also the problem in Equation (24) satisfies the convexity and concavity properties that we need. Hence, both problems in Equations (24),(28) have a unique solution. Finally, note that the optimum  $\delta^*$  in Equation (32) satisfies  $\delta^* = \frac{1}{\sqrt{d}} \|\Pi_{\perp} \theta\|$ , and similarly the optima  $\nu_{\perp}^*$  and  $\nu_{\parallel}^*$  in Equation (35) satisfy  $\nu_{\perp}^* = \|\Pi_{\perp} \theta\|_2$  and  $\nu_{\parallel}^* = \langle \theta, \theta^* \rangle$ . We can therefore conclude the proof as the solutions of the optimization problems (24), (28) concentrate asymptotically around the same optima as  $d, n \rightarrow \infty$ .

## F.2 Proof of Theorem F.2

Recall the robust max-margin solution from Equation (8):

$$\min_{\theta, \delta} \|\theta\|_2^2 \quad \text{such that } \langle \theta, x_i \rangle - \delta \geq 1 \text{ for all } i \text{ and } \epsilon \|\Pi_{\perp} \theta\|_1 = \delta \quad (38)$$

Like in the previous section, after introducing the Lagrange multipliers  $\zeta$  and  $u$  we can equivalently write

$$\min_{\theta, \delta} \max_{\substack{u: u_i \geq 0, \\ \zeta \geq 0}} \|\theta\|_2^2 + \frac{1}{n} u^{\top} (1 + 1\epsilon_0 \delta - D_y \text{X}\theta) + \zeta \left( \frac{\|\Pi_{\perp} \theta\|_1}{\sqrt{d}} - \delta \right), \quad (39)$$

and again separating  $\text{X} = \text{XII}_{\perp} + \text{XII}_{\parallel}$ , we get

$$\min_{\theta, \delta} \max_{\substack{u: u_i \geq 0, \\ \zeta \geq 0}} \|\theta\|_2^2 + \frac{1}{n} u^{\top} (1 + 1\epsilon_0 \delta - D_y \text{XII}_{\parallel} \theta - D_y \text{XII}_{\perp} \theta) + \zeta \left( \frac{\|\Pi_{\perp} \theta\|_1}{\sqrt{d}} - \delta \right). \quad (40)$$

**Convex Gaussian Minimax Theorem** Since the adversarial attacks are consistent and the observations are noiseless, we know the solution in Equation (38) exists for all  $d, n$ . Yet, in order to apply the CGMT, we have to show that we can restrict  $u$  and  $\theta$  to compact sets. This follows from a simple trick as explained in Section D.3.1 in [24]. Hence, the primal optimization problem from Equation (40) can be asymptotically replaced with the following auxiliary optimization problem, where, as before,  $g \in \mathbb{R}^d$  and  $h \in \mathbb{R}^n$  are random vectors with i.i.d. standard normal entries:

$$\begin{aligned}
& \min_{\theta, \delta} \max_{\substack{u: u_i \geq 0, \\ \zeta \geq 0}} \|\theta\|_2^2 + \frac{1}{n} u^{\top} (1 + 1\epsilon_0 \delta - D_y \text{XII}_{\parallel} \theta + D_y h \|\Pi_{\perp} \theta\|_2) \\
& \quad + \frac{1}{n} \|u\|_2 g^{\top} \Pi_{\perp} \theta + \zeta \left( \frac{\|\Pi_{\perp} \theta\|_1}{\sqrt{d}} - \delta \right). \quad (41)
\end{aligned}$$



**Scalarization of the optimization problem** The goal is again to scalarize the optimization problem. As a first step, we can solve the optimization over  $u$  when defining  $r = \frac{\|u\|_2}{\sqrt{n}}$ :

$$\begin{aligned} & \min_{\theta, \delta \geq 0} \max_{\substack{r \geq 0, \\ \zeta \geq 0}} \|\theta\|_2^2 + \frac{r}{\sqrt{n}} \|\max(0, 1 + 1\epsilon_0\delta - D_y X \Pi_{\parallel} \theta + D_y h \|\Pi_{\perp} \theta\|_2)\|_2 \\ & \quad + \frac{r\sqrt{\gamma}}{\sqrt{d}} g^{\top} \Pi_{\perp} \theta + \zeta \left( \frac{1}{\sqrt{d}} \|\Pi_{\perp} \theta\|_1 - \delta \right), \end{aligned}$$

where  $\max$  applies element-wise over the vector. We can now swap maximization and minimization since the objective is convex in  $\theta, \delta$  and concave in  $r$ :

$$\begin{aligned} & \max_{\substack{r \geq 0, \\ \zeta \geq 0}} \min_{\theta, \delta \geq 0} \|\theta\|_2^2 + \frac{r}{\sqrt{n}} \|\max(0, 1 + 1\epsilon_0\delta - D_y X \Pi_{\parallel} \theta + D_y h \|\Pi_{\perp} \theta\|_2)\|_2 \\ & \quad + \frac{r\sqrt{\gamma}}{\sqrt{d}} g^{\top} \Pi_{\perp} \theta + \zeta \left( \frac{1}{\sqrt{d}} \|\Pi_{\perp} \theta\|_1 - \delta \right). \end{aligned}$$

We now want to separate  $\|\Pi_{\perp} \theta\|_2$  from the term in  $\max$ . This is achieved by introducing the variable  $\nu_{\perp} \geq 0$  and the Lagrange multiplier  $\kappa$ . Further, we set  $\nu_{\parallel} = \langle \theta^*, \Pi_{\parallel} \theta \rangle$  (recall that  $\theta^* = (1, 0, \dots, 0)$ ), which allows us to equivalently write

$$\begin{aligned} & \max_{\substack{r \geq 0, \\ \zeta \geq 0}} \min_{\substack{\nu_{\perp} \geq 0, \\ \nu_{\parallel}, \delta \geq 0, \Pi_{\perp} \theta}} \max_{\kappa \geq 0} \nu_{\parallel}^2 + \|\Pi_{\perp} \theta\|_2^2 + \kappa (\|\Pi_{\perp} \theta\|_2 - \nu_{\perp}) \\ & \quad + \frac{r}{\sqrt{n}} \|\max(0, 1 + 1\epsilon_0\delta - D_y X \Pi_{\parallel} \theta^* \nu_{\parallel} + D_y h \nu_{\perp})\|_2 \\ & \quad + \frac{r\sqrt{\gamma}}{\sqrt{d}} g^{\top} \Pi_{\perp} \theta + \zeta \left( \frac{1}{\sqrt{d}} \|\Pi_{\perp} \theta\|_1 - \delta \right). \end{aligned} \quad (42)$$

Next, we use again the trick  $\min_{\tau \geq 0} \frac{x^2}{2\tau} + \frac{\tau}{2} = x$ , which yields

$$\begin{aligned} & \max_{\substack{r \geq 0, \\ \zeta \geq 0}} \min_{\substack{\nu_{\perp} \geq 0, \\ \nu_{\parallel}, \delta \geq 0, \Pi_{\perp} \theta}} \max_{\kappa \geq 0} \min_{\tau \geq 0} \nu_{\parallel}^2 + \|\Pi_{\perp} \theta\|_2^2 - \kappa \nu_{\perp} + \frac{\kappa}{2\tau} \|\Pi_{\perp} \theta\|_2^2 \\ & \quad + \frac{\kappa\tau}{2} + \frac{r}{\sqrt{n}} \|\max(0, 1 + 1\epsilon_0\delta - D_y X \Pi_{\parallel} \theta^* \nu_{\parallel} + D_y h \nu_{\perp})\|_2 \\ & \quad + \frac{r\sqrt{\gamma}}{\sqrt{d}} g^{\top} \Pi_{\perp} \theta + \zeta \left( \frac{1}{\sqrt{d}} \|\Pi_{\perp} \theta\|_1 - \delta \right). \end{aligned} \quad (43)$$

In a next step, note that due to high dimensional concentration, we have that

$$\begin{aligned} & \frac{r}{\sqrt{n}} \|\max(0, 1 + 1\epsilon_0\delta - D_y X \Pi_{\parallel} \theta^* \nu_{\parallel} + D_y h \nu_{\perp})\|_2 \\ & \stackrel{\text{LLN}}{\rightarrow} r \sqrt{\mathbb{E}_{Z_{\parallel}, Z_{\perp}} \left[ \max(0, 1 + \epsilon_0\delta - |Z_{\parallel}| \nu_{\parallel} + Z_{\perp} \nu_{\perp})^2 \right]} =: \sqrt{T}, \end{aligned}$$

where  $Z_{\parallel}, Z_{\perp}$  are standard Gaussian distributed random variable. Next, by completion of the squares we get

$$\begin{aligned} & \max_{\substack{r \geq 0, \\ \zeta \geq 0}} \min_{\substack{\nu_{\perp} \geq 0, \\ \nu_{\parallel}, \delta \geq 0, \Pi_{\perp} \theta}} \max_{\kappa \geq 0} \min_{\tau \geq 0} \nu_{\parallel}^2 + \left(1 + \frac{\kappa}{2\tau}\right) \|\Pi_{\perp} \theta\|_2^2 + \frac{r\sqrt{\gamma}}{\sqrt{d}2\left(1 + \frac{\kappa}{2\tau}\right)} g^{\top} \Pi_{\perp} \theta \\ & \quad - \kappa \nu_{\perp} + \sqrt{T} + \zeta \left( \frac{1}{\sqrt{d}} \|\Pi_{\perp} \theta\|_1 - \delta \right) + \frac{\kappa\tau}{2} \end{aligned}$$

with  $\|g/\sqrt{d}\|_2^2 \rightarrow 1$ . Next, note that we can again swap minimization and maximization due to the

convexity and concavity, respectively, of the optimization. Hence, we can rewrite

$$\begin{aligned} \max_{\substack{r \geq 0, \\ \zeta \geq 0}} \min_{\substack{\nu_{\perp} \geq 0, \\ \nu_{\parallel}, \delta \geq 0}} \max_{\kappa \geq 0} \min_{\tau \geq 0, \Pi_{\perp} \theta} \nu_{\parallel}^2 + (1 + \frac{\kappa}{2\tau}) \|\Pi_{\perp} \theta + \frac{r\sqrt{\gamma}}{\sqrt{d}2(1 + \frac{\kappa}{2\tau})} g\|_2^2 - \frac{r^2\gamma}{4(1 + \frac{\kappa}{2\tau})} \|g/\sqrt{d}\|_2^2 \\ - \kappa\nu_{\perp} + \sqrt{T} + \zeta \left( \frac{1}{\sqrt{d}} \|\Pi_{\perp} \theta\|_1 - \delta \right) + \frac{\kappa\tau}{2}. \end{aligned}$$

Finally, to obtain the desired optimization problem, we only need to solve the inner optimization over  $\Pi_{\perp} \theta$ . For this, we can write:

$$\begin{aligned} \min_{\Pi_{\perp} \theta} (1 + \frac{\kappa}{2\tau}) \|\Pi_{\perp} \theta + \frac{r\sqrt{\gamma}}{\sqrt{d}2(1 + \frac{\kappa}{2\tau})} g\|_2^2 + \zeta \frac{\|\Pi_{\perp} \theta\|_1}{\sqrt{d}} \\ \stackrel{\tilde{\theta}_{\perp} = \frac{\Pi_{\perp} \theta}{\sqrt{d}}}{=} \min_{\tilde{\theta}_{\perp}} \frac{1}{d} (1 + \frac{\kappa}{2\tau}) \|\tilde{\theta}_{\perp} + \frac{r\sqrt{\gamma}}{2(1 + \frac{\kappa}{2\tau})} g\|_2^2 + \zeta \frac{\|\Pi_{\perp} \theta\|_1}{d} \\ = \frac{1}{d} \sum_{i=2}^d \min_{(\tilde{\theta}_{\perp})_i} (1 + \frac{\kappa}{2\tau}) \left( (\tilde{\theta}_{\perp})_i + \frac{r\sqrt{\gamma}}{2(1 + \frac{\kappa}{2\tau})} g_i \right)^2 + \zeta |(\tilde{\theta}_{\perp})_i| \\ = \frac{1}{d} 2(1 + \frac{\kappa}{2\tau}) \sum_{i=2}^d \min_{(\tilde{\theta}_{\perp})_i} \frac{1}{2} \left( (\tilde{\theta}_{\perp})_i + \frac{r\sqrt{\gamma}}{2(1 + \frac{\kappa}{2\tau})} g_i \right)^2 + \frac{\zeta}{2(1 + \frac{\kappa}{2\tau})} |(\tilde{\theta}_{\perp})_i| \\ = \frac{1}{d} 2(1 + \frac{\kappa}{2\tau}) \sum_{i=2}^d \ell_{\text{H}} \left( -\frac{r\sqrt{\gamma}}{2(1 + \frac{\kappa}{2\tau})} g_i, \frac{\zeta}{2(1 + \frac{\kappa}{2\tau})} \right) \\ \rightarrow 2(1 + \frac{\kappa}{2\tau}) \mathbb{E}_Z \ell_{\text{H}} \left( \frac{r\sqrt{\gamma}}{2(1 + \frac{\kappa}{2\tau})} Z, \frac{\zeta}{2(1 + \frac{\kappa}{2\tau})} \right) \end{aligned}$$

where we solve the optimization in the fourth line with  $\ell_{\text{H}}$  being the Huber loss, given by  $\ell_{\text{H}}(x, y) = \begin{cases} 0.5x^2 & |x| \leq y \\ y(|x| - 0.5y) & |x| > y \end{cases}$ .

Finally, we can conclude the proof from

$$\mathbb{E}_Z \ell_{\text{H}}(aZ, b) = \frac{a^2 + b^2}{2} \text{erf} \left( \frac{b}{\sqrt{2}a} \right) - \frac{b^2}{2} + \frac{ab}{\sqrt{2\pi}} \exp \left( -\frac{b^2}{2a^2} \right).$$

**Convergence** One can check that the optimization problems defined in Equations (26),(40) are convex in the variables which we minimize over and concave in the variables which we maximize over. Indeed, Equation (40) is immediate and Equation (26) follows straightforwardly, like before, from the fact that the desired convexity and concavity are satisfied for the problem defined in Equation (43). Thus, both problems defined in Equations (26),(40) have unique solutions. We note again that the optimum  $\delta^*$  in Equation (39) satisfies  $\delta^* = \frac{1}{\sqrt{d}} \|\Pi_{\perp} \theta\|$ , and similarly the optima  $\nu_{\perp}^*$  and  $\nu_{\parallel}^*$  in Equation (43) satisfy  $\nu_{\perp}^* = \|\Pi_{\perp} \theta\|_2$  and  $\nu_{\parallel}^* = \langle \theta, \theta^* \rangle$ . Hence we can conclude the proof as the solutions of problems (26), (40) concentrate asymptotically as  $d, n \rightarrow \infty$  around the same optima.